**Journal of Umm Al-Qura University for Applied Science**

**journal homepage:** https://uqu.edu.sa/en/jas/87823

# Quantum Mechanical Stark Broadening for Na VII and Na VIII lines

**Haykel Elabidi** [a,b].

[a] *Common First Year Deanship, Physics Department, Umm Al-Qura University, Makkah, Saudi Arabia.*
[b] *Laboratory of Molecular Spectroscopy and Dynamics, Sciences Faculty of Bizerte, Carthage University, Tunisia.*

**ARTICLE INFO**

***Article History:***
Submission date: 16/9/2019
Accepted date: 22/6/2020

***Keywords:***
*line profiles, atomic data, scattering*

**ABSTRACT**

*We theoretically investigated the structure, the collisional and the Stark broadening problems of the two ions Na VII and Na VIII. We used our quantum mechanical method to calculate new electron impact widths for 20 Na VII and 20 Na VIII spectral lines. No line widths for the two ions have been found in the literature, so no comparisons have been done for this part. Results are provided for electron density $N_e = 10^{17}$ $cm^{-3}$ and for electron temperatures from $2 \times 10^5$ K to $10^6$ K. We also calculate the radiative and the collisional atomic data. These intermediate results are used for the evaluation of the line broadening, and consequently, their examination are primordial for testing our line broadening accuracy. We extensively compared all of our intermediate results with several theoretical and experimental ones. We found in general acceptable agreements between them, which could guarantee the precision of our line broadening calculations since there are no comparisons for them. The presented data are useful for the diagnostics and modelling of laboratory and astrophysical plasmas.*

## 1. Introduction

Atomic data represent an important tool in the diagnostics of the physical properties of plasmas such as temperature and density, and for the interpretation of astronomical spectra. For instance, the Einstein coefficients are calculated in several kinetic processes using radiative decay rates. Radiative decay rates are also used in the evaluation of lifetimes which are measurable quantities. In many works [1], the authors calculated oscillator strengths to include in their models radiative and collisional bound-bound transitions. Another particular use of energy levels is in the Stark broadening evaluation for some methods such as the semiclassical and the semi-empirical ones. Furthermore, the study of the line intensities needs the knowledge of all the excitation/ de-excitation processes contributing to the intensity. Consequently, electron collision strengths are used in the calculations of level population and line intensities. The Stark broadening mechanism is also important in many astrophysical applications. Line broadening data for many ions are missing in the literature, and this lack represents an obstacle for the analysis by means of NLTE model atmospheres. These techniques have been quickly developed and improved so that we can not fulfill their need to the atomic data. On the other side, atomic data and Stark broadening tables of many ions are missing. The lack of line broadening data is noteworthy for heavy and highly charged ions, furthermore, when the data are not calculated for suitable temperatures, the abundance determination will not be sufficiently accurate. To use these data correctly, they should be extrapolated to the desired temperatures. That extrapolation procedure causes also an inaccuracy in the abundance determination, because the relation between line widths and temperature is not well established. In some cases, it is necessary to calculate the line broadening of a large number of species (atoms and their ions). This occurs when calculating the opacity and radiative transfer [2,3]. Recently, it has been shown that we need models that include the opacities of heavy element to analyze white dwarf atmospheres [4]. It has been shown also that Stark broadening contribution dominates that of the Doppler one.

The two ions studied in the present work are the boron-like Na VII and the beryllium-like Na VIII. B-like ions are very important for modelling of astrophysical and laboratory plasmas. Their lines have been observed and studied in the seventeens [5-8]. Recently, many extensive calculations for structure and radiative data have been performed. In the newest work, the multiconfiguration Dirac–Fock (MCDF) method including QED corrections has been applied on many isoelectronic sequence (including B-like) of the ions Nd, Sm, Gd, Dy, Er, and Yb [9]. Another extensive calculations for the Be-like ($Z = 4 - 12$) to the Ne-like ($Z = 10 - 24$) sequences including the Boron isoelectronic one have been performed by Froese Fischer & Tachiev [10]. For the Na VII ion, Jönsson *et al.* [11] have recently presented relativistic configuration interaction (RCI) calculations of lifetimes, energy levels, wavelengths, transitions probabilities, oscillator strengths and relative intensities of lines. Their calculations are based on multiconfiguration Dirac–Hartree–Fock (MCDHF) wave functions. They performed also an extensive comparisons with the available results. A detailed list of the earlier works dedicated to the atomic calculations of B-like ions and specially to the Na VII ion can be found in Jönsson *et al.* [11]. Be-like ions are also of interest in laboratory and astrophysical plasmas because they emit in wide range of wavelengths. Their lines have been observed in solar atmosphere and stellar planetary nebulae. The most complete systematic structure calculations for the beryllium isoelectronic sequence ($10 \leq Z \leq 30$) has been performed by Wang *et al.* [12]. Many other works have been published before but including only configurations with $n \leq 2$ [13-17], and other works where the used configurations include up to $n = 3$ [10,18,19]. In another report [15], the authors have taken into account configurations with $n$ up to 5. The collision problem for B-like ions with atomic number $Z$ from 8 to 92 has been treated in the frame of the relativistic distorted wave approximation [20], where collision strengths and oscillator strengths have been calculated for transitions involving only levels with the same principal quantum number $n = 2$. The same method [20] has been applied on the Be-like ions with $8 \leq Z \leq 92$ [21]. R-matrix calculations for excitation collision strengths have been carried out for B-like ions from carbon to Krypton [22], and for Be-like ions from Boron to Zinc [23]. In the two last works, the results have been presented as effective collision strengths $\Upsilon$ (collision strengths averaged over the Maxwellian energy distribution). In spite of the importance of the two ions studied here, and even though their radiative atomic and collisional data exist, experimental and theoretical Stark broadening data are totally missing.

The atomic data are evaluated in the present work using the SUPERSTRUCTURE code (SST) [24]. The collision part is carried out using the two UCL codes DISTORTED WAVE (DW) [25] and JAJOM [26,27]. A short description of the codes will be given hereafter. We use here our quantum mechanical approach for the Stark broadening calculations. The quantum mechanical expression calculating electron impact broadening has been obtained by Elabidi *et al.* [28,29]. The expression is established in intermediate coupling for the atomic structure and under the impact approximation. We have applied this approach for Be-like ions from carbon to neon [29]. Stark broadening of the Li-like ions from carbon to phosphorus has been

studied [30], where in addition, the influence of fine structure effects on line broadening has been investigated. We have also used our method to investigate some regularities of line widths [31]. Elabidi *et al.* [32] studied the strong collisions and their contributions to line broadening. Quantum Stark broadening data of Ar VII lines have been provided by Aloui *et al.*[33], where extensive analysis and comparisons with semiclassical results have been performed interpreting some discrepancies found between the two approaches. Using our method and a fitting procedure applied on the two ions Ar V and Ar VI, we have proposed a temperature dependence of line widths [34]. We have used an analogous fitting method applied on some N-like ions from sodium to silicon to establish a density dependence of line widths [35]. In another report [36], new Stark broadening data of Ar VIII and Ar IX lines have been provided and the results of Ar VIII have been compared to those of the semiclassical approach [37], and a comparison between the importance of Stark and Doppler broadening in the atmospheric conditions of DO white dwarfs has been performed. In all the above cited works, and in the cases where there are comparisons, our quantum results showed acceptable agreements with the other experimental or theoretical ones. In many other cases, our results are the first to be published and thus contribute to fulfill the lack of line broadening data.

Here we have calculated Stark broadening for 20 Na VII and 20 Na VIII spectral lines. As far as we know, the line widths studied in the present work have not been calculated before. We calculated also all the necessary radiative data (energy levels, lifetimes, radiative decay rates, oscillator strengths and line strengths). We calculated also collision strengths for several electron energies ranging from the excitation threshold region of the corresponding transition to energies far from this threshold. We investigated the convergence of the collision strengths with electron energy. Comparisons have been performed with available results, and acceptable agreements have been found. This conclusion gives us confidence in our intermediate results used in the line broadening calculations. We hope that our work participates with other ones to fill in the lack of line broadening data.

## 2. Theory

### *2.1. Atomic structure and radiative data*

The SST code starts by calculating the eigenfunctions of the operators $L^2$, $L_z$, $S^2$ and $S_z$ using the Slater state expansion method described by Condon & Shortley [38]. The obtained eigenfunctions are then used to calculate the matrix elements of the non relativistic many–electron Hamiltonian, which provide the term energies and the radiative data between these terms (radiative data in *LS* coupling). The relativistic effects are introduced through the Breit–Pauli Hamiltonian [39], where the same eigenfunctions are used to evaluate the matrix elements of the relativistic operators in the Breit–Pauli Hamiltonian [40,41]. SST takes into account the mass-variation, the one–body Darwin and the two–body fine structure interactions. The two-body non–fine structure effects are neglected. This provides fine structure energy levels (defined by the quantum numbers corresponding to the operators $L^2$, $S^2$, $J^2$ and $J_z$) and radiative data in intermediate coupling. The calculations include electric dipole/quadripole and magnetic dipole transitions. SST supplies also the term-coupling coefficients (TCC) used in JAJOM code [26,27] to take into account intermediate coupling effects in the collision problem (see next subsection). The radial wave functions are evaluated here within the SST program (there is another option that these functions can be introduced by the user as an input). They are determined by diagonalization of the non relativistic Hamiltonian using orbitals calculated in a scaled Thomas–Fermi–Dirac Amaldi (TFDA) potentials. The potential depends on scaling parameters $\lambda_l$ that have been obtained by a self–consistent energy minimization on the term energies included in our calculations.

### *2.2. Electron-ion scattering*

The collision strength can be defined as the measure of strength for a binary collision. It contains the information about this collision. It is a dimensionless quantity and is related to the collision cross section $\sigma$ by the following relationship:

$$\Omega_{if} = \frac{k_i^2 g_i}{\pi a_0^2}\sigma_{if}, \qquad (1)$$

where $k_i^2$ is the incident electron energy in Ryd and $g_i$ is the statistical weight of the initial level. We can say also that both collision strength and cross section describe the intrinsic probability of collisional excitation and de-excitation in an atomic transition at a particular electron energy, but collision strength is preferred because it is symmetric in the initial and final levels.

The collision study starts by calculating the reactance matrices $\mathfrak{R}$ and collision strengths $\Omega$ in $LS$ coupling where the distorted wave approximation is assumed. This is done in our work through the code DISTRORTED WAVE [25]. Collision strengths in intermediate coupling, including relativistic effects, are evaluated in the JAJOM code [26,27]. In fact, when the nuclear charge increases and for high ionization stages, the contributions of the relativistic effects become important and hence they have to be taken into account when calculating collision strengths. The basic idea of JAJOM is to transform collision parameters form the $LS$ coupling to the intermediate one taking into account these relativistic interactions in the structure study. The adopted procedure in JAJOM consists on calculating, in a first stage, the collision strengths in $LS$ coupling from the reactance matrices $\mathfrak{R}^{SL}$ obtained in DISTRORTED WAVE:

$$\Omega(\Gamma_i S_i L_i, \Gamma'_i S'_i L'_i) = \tfrac{1}{2}\textstyle\sum_{SL\pi}\sum_{ll'}(2S+1)(2L+1)|T^{SL\pi}(\Gamma_i S_i L_i ls, \Gamma'_i S'_i L'_i l's)|^2. \qquad (2)$$

$T$ is the transition matrix related to the reactance one by $T = 2i\mathfrak{R}(I - i\mathfrak{R})^{-1}$; $I$ is unit matrix. Capital letters refer to the quantum numbers of the emitter, $l$ and $s$ refer to those of the scattered electron and $\pi = (-1)^{\Sigma l}$ is the parity of the hole system (emitter+electron). Γ is a configuration parameter. In a second step, the reactance matrices $\mathfrak{R}^{SL}$ are transformed into $JK$ coupling schema defined by: $L_j$+$S_j$=$J_j$, $J_j$+$l$=$K_j$, $K_j$+$s$=$J$. The reactance matrices in $JK$ coupling are given by (Saraph 1972)[26]:

$$\mathfrak{R}^{J\pi}(\Gamma_i S_i L_i J_i lK; \Gamma'_i S'_i L'_i J'_i l'K'; \varepsilon) = \textstyle\sum_{SL} C(SLJ; S_i L_i J_i; lK)\mathfrak{R}^{SL\pi}(\Gamma_i S_i L_i ls; \Gamma'_i S'_i L'_i l's; \varepsilon) C(SLJ; S'_i L'_i J'_i; l'K'), \qquad (3)$$

where $C$ are the re-coupling coefficients of Racah (1943) [42]. Finally, the matrices $\mathfrak{R}^{J\pi}$ are then transformed into intermediate coupling $\mathfrak{R}^{IC}$. The last transformation needs the TCC: $f_{J_i}(\Delta_i, \Gamma_i S_i L_i)$ defined in the previous reports [24,26] and obtained in SST:

$$\mathfrak{R}^{IC}(\Delta_i J_i lK, \Delta'_i J'_i l'K') = \textstyle\sum_{S_i L_i}\sum_{S'_i L'_i} f_{J_i}(\Delta_i, \Gamma_i S_i L_i)\mathfrak{R}^{J\pi} f_{J'_i}(\Delta'_i, \Gamma'_i S'_i L'_i J'_i). \qquad (4)$$

The parameters $\Delta_i$ replace the set of the quantum numbers $\Gamma_i S_i L_i$. The collision strengths are then obtained from $\mathfrak{R}^{IC}$ in the same way as in (2):

$$\Omega(\Delta_i J_i - \Delta'_i J'_i) = \textstyle\sum_{ll'KK'}\sum_{J\pi}\frac{(2J+1)}{2}\left|T^{J\pi}_{ic}(\Delta_i J_i lK; \Delta'_i J'_i l'K')\right|^2. \qquad (5)$$

During this procedure, it is assumed that the reactance matrices are independent of energy. The obtained parameters will be used later in the line broadening evaluation.

### *2.3. Line broadening calculations*

Our quantum mechanical line broadening method used here is a combination between the line broadening and the collision theories. Our line broadening method has three stages: the structure and collision calculations are the the two first stages and represent the start-up step of the line broadening treatment. In the third stage, the parameters obtained from the two first ones (energy levels, reactance matrices, scattering matrices,..) are adequately arranged and adapted to be used in the line broadening calculations through the codes JAJPOLARI (Dubau, unpublished results) and RtoS (Elabidi & Dubau, unpublished results). JAJPOLARI is a transformed version of JAJOM, it extracts the reactance matrices $\mathfrak{R}$ from JAJOM. These matrices which will be used to calculate the real and imaginary parts of scattering matrices $\mathbb{S}$ through the code RtoS:

$$\mathbb{S} = \frac{I+i\mathfrak{R}}{I-i\mathfrak{R}}, \qquad (6)$$

and

$$Re\ \mathbb{S} = (I-\mathfrak{R}^2)(I+\mathfrak{R}^2)^{-1}, Im\ \mathbb{S} = 2\mathfrak{R}(I+\mathfrak{R}^2)^{-1}. \qquad (7)$$

The original expression of the quantum full width corresponding to a transition $i \longrightarrow f$ under the assumption of the impact approximation has been given by the following equation [43]:

$$W = 2N_e\int_0^\infty vf(v)\left(\textstyle\sum_{i'\neq i}\sigma_{ii'}(v) + \sum_{f'\neq f}\sigma_{ff'}(v) + \int\left|f_i(\theta,v) - f_f(\theta,v)\right|^2 \mathrm{d}\Omega\right)dv, \qquad (8)$$

where $N_e$ is the electron density and $v$ is the velocity of the perturbing electron. $\sigma$ are the inelastic cross sections connecting the levels $i$ and $f$ involved in the transition to their perturbing ones. The integral over the scattering angle $\theta$ represents the elastic part of the collision. $d\Omega$ is the element of solid angle and $f(v)$ is the Maxwellian electron velocity distribution given by:

$$\text{with} \qquad f(v) = 4\pi\left(\frac{m}{2\pi k_B T_e}\right)^{\frac{3}{2}} v^2 \exp\left(-\frac{mv^2}{2k_B T_e}\right); \qquad (9)$$
$$\int f(v)dv = 1,$$

$m$ is the electron mass, $T_e$ the electron temperature and $k_B$ the Boltzmann constant.

The expression of the quantum mechanical full Stark width in intermediate coupling has been derived in the previous reports [28,29]. The principal assumption in our method is the impact approximation:

$$W = \qquad (10)$$
$$2N_e\left(\frac{\hbar}{m}\right)^2\left(\frac{2m\pi}{k_B T_e}\right)^{\frac{1}{2}}\int_0^\infty \Gamma_w(\varepsilon)\exp\left(-\frac{\varepsilon}{k_B T_e}\right)d\left(\frac{\varepsilon}{k_B T_e}\right),$$

where

$$\Gamma_w(\varepsilon) = \sum_{J_i^T J_f^T l K_i K_f} \frac{[K_i,K_f,J_i^T,J_f^T]}{2}\begin{Bmatrix} J_i & K_i & l \\ K_f & J_f & 1\end{Bmatrix}^2\begin{Bmatrix} K_i & J_i^T & s \\ J_f^T & K_f & 1\end{Bmatrix}^2 \qquad (11)$$
$$\times\left[1-\left(\mathrm{Re}\,(\mathbb{S}_i)\mathrm{Re}\,(\mathbb{S}_f)+\mathrm{Im}\,(\mathbb{S}_i)\mathrm{Im}\,(\mathbb{S}_f)\right)\right].$$

Uppercase letters refer to the quantum operators of the emitter (the considered ion), the lowercase ones refer to those of the incident electron and letters with the superscript $T$ are the operators of the emitter+electron system. $\mathrm{Re}\,(\mathbb{S})$ and $\mathrm{Im}\,(\mathbb{S})$ are the real and the imaginary parts of the scattering matrix which are expressed in the intermediate coupling schema. The terms in braces represent the 6–j symbols and the notation $[K_i,K_f,J_i^T,J_f^T]$ means $(2K_i+1)\times(2K_f+1)\times(2J_i^T+1)\times(2J_f^T+1)$. The scattering matrices $\mathbb{S}$ and their real and imaginary parts calculated in RtoS are arranged in an adequate order as input data suitable for the formula (11). Finally, we obtain the line width when the sum in (11) and the integral in (10) are performed.

## 3. Results and discussions

### *3.1. Atomic structure and collision data*

We recall that the lifetime $\tau$ for a level $j$ is given by:

$$\tau_j = \frac{1}{\sum_i A_{ji}} \qquad (12)$$

where $A_{ji}$ is the radiative decay rates from the level $j$ to all the possible lower levels $i$. The radiative decay rates and the absorption oscillator strengths are related to the line strength $S^{[E1]}$ for electric dipole transitions by:

$$\text{and } A_{ji} = 2.6774\times10^9\frac{(\Delta E)^3}{g_j}S^{[E1]}, \qquad (13)$$
$$f_{ij} = \frac{\Delta E}{3g_i}S^{[E1]}, \qquad (14)$$

here $S^{[E1]}$ is expressed in power of Bohr radii $a_0$ and $A_{ji}$ is given in units inverse to the Rydberg time $\tau_0 = 4.838\times10^{17}$ s. $\Delta E$ is the transition energy in Rydbergs and $g_i$ and $g_j$ are the statistical weights of the lower $(i)$ and upper $(j)$ levels, respectively.

For the B-like sodium (Na VII), we have included in the calculations 8 configurations: 1s$^2$ [2s$^2$2p, 2s2p$^2$, 2p$^3$, 2s$^2$3s, 2s$^2$3p, 2s$^2$3d, 2s2p3s, 2s2p3p]. This set of configurations gives rise to 23 terms and 45 fine structure levels. The energies of the 45 fine structure levels are presented along with their lifetimes in Tables 1 and 2. Extensive comparisons have been performed for all the data presented here. Energies are compared to the NIST [44] values, to the RCI ones of Jönsson *et al.* [11], and to other relativistic (Koc) results [45]. The averaged agreement is acceptable and doesn't exceed 2 per cent. We note that some of our levels are inverted regarding to those from the database NIST. In almost all these cases, the inversion is between $^2$D$_{3/2}$ and $^2$D$_{5/2}$ levels. The lifetimes have been compared to the experimental results of Buchet *et al.* [46], Tordoir *et al.*[47] when available, otherwise, they are compared to the relativistic configuration interaction (RCI) results of Jönsson *et al.* [11]. The two comparisons show an agreement of about 20 per cent over all the levels.

**Table 1:** Our energy levels $E$ in cm$^{-1}$ and lifetimes $\tau$ in s for Na VII are compared to the Relativistic Configuration Interaction (RCI) calculations [11], to other relativistic (Koc) results (Koc 2003) [44] and to those of NIST [44] database. Lifetimes are compared also to the experimental results of Buchet *et al.* (1978) [46], Tordoir *et al.* [47]. Levels marked by (∗) are inverted regrading to the NIST ones. aE−b means $a\times10^{-b}$.

| Index | Conf. | Level | $E$ | NIST | RCI | Koc | $\tau$ | $\tau_{\mathrm{RCI}}$ | $\tau_{Koc}$ | $\tau_{exp}$ |
|---|---|---|---|---|---|---|---|---|---|---|
| 1 | 2s $^2$2p | $^2$P $^o_{1/2}$ | 0 | 0 | 0 | 0 | – | – | – | – |
| 2 | 2s $^2$2p | $^2$P $^o_{3/2}$ | 2195. | 2134.61 | 2134 | 2138 | – | – | – | – |
| 3 | 2s2p $^2$ | $^4$P $_{1/2}$ | 109481. | 114995 | 114856 | 114878 | – | – | – | – |
| 4 | 2s2p $^2$ | $^4$P $_{3/2}$ | 110258. | 115728 | 115572 | 115618 | – | – | – | – |
| 5 | 2s2p $^2$ | $^4$P $_{5/2}$ | 111520. | 116798 | 116652 | 116668 | – | | – | – |
| 6 * | 2s2p $^2$ | $^2$D $_{3/2}$ | 210887. | 205448 | 205485 | 205681 | 6.397E−10 | 7.146E−10 | 7.111E−10 | 6.90E−10 |
| 7 * | 2s2p $^2$ | $^2$D $_{5/2}$ | 210918. | 205412 | 205444 | 205617 | 6.597E−10 | 7.384E−10 | 7.350E−10 | 7.00E−10 |
| 8 | 2s2p $^2$ | $^2$S $_{1/2}$ | 269062. | 264400 | 264501 | 264760 | 1.303E−10 | 1.618E−10 | 1.615E−10 | 1.55E−10 |
| 9 | 2s2p $^2$ | $^2$P $_{1/2}$ | 297759. | 283869 | 283975 | 284147 | 7.181E−11 | 8.355E−11 | 8.335E−11 | 7.30E−11 |
| 10 | 2s2p $^2$ | $^2$P $_{3/2}$ | 299236. | 285189 | 285291 | 285465 | 7.142E−11 | 8.311E−11 | 8.283E−11 | – |
| 11 | 2p $^3$ | $^4$S $^o_{3/2}$ | 365953. | 367308 | 367189 | 367240 | 8.245E−11 | 9.249E−11 | 9.242E−11 | 9.50E−11 |
| 12 * | 2p $^3$ | $^2$D $^o_{3/2}$ | 424125. | 412311 | 412321 | 412533 | 2.355E−10 | 2.859E−10 | 2.856E−10 | – |
| 13* | 2p $^3$ | $^2$D $^o_{5/2}$ | 424175. | 412395 | 412407 | 412641 | 2.346E−10 | 2.850E−10 | 2.852E−10 | 2.80E−10 |

**Table 2:** Same as in Table 1 but without experiemntal lifetimes $\tau$.

| Index | Conf. | Level | $E$ | NIST | RCI | Koc | $\tau$ | $\tau_{\mathrm{RCI}}$ | $\tau_{\mathrm{Koc}}$ |
|---|---|---|---|---|---|---|---|---|---|
| 14 | 2p $^3$ | $^2$P $^o_{1/2}$ | 478851. | 465017 | 465155 | 465406 | 9.420E−11 | 1.162E−10 | 1.163E−10 |
| 15 | 2p $^3$ | $^2$P $^o_{3/2}$ | 479005. | 465111 | 465247 | 465509 | 9.458E−11 | 1.167E−10 | 1.167E−10 |
| 16 | 2s $^2$3s | $^2$S $_{1/2}$ | 968044. | 951350 | 951183 | 951067 | 2.008E−11 | 2.024E−11 | 2.027E−11 |
| 17 | 2s $^2$3p | $^2$P $^o_{1/2}$ | 1027578. | – | 1007786 | 1007696 | 1.162E−10 | 2.217E−10 | 2.244E−10 |
| 18 | 2s $^2$3p | $^2$P $^o_{3/2}$ | 1028071. | 1008420 | 1008332 | 1008252 | 1.155E−10 | 2.227E−10 | 2.238E−10 |
| 19 * | 2s2p($^3$P)3s | $^4$P $^o_{1/2}$ | 1073881. | 1077270 | 1077041 | 1077012 | 2.757E−11 | 1.684E−11 | 1.690E−11 |
| 20 | 2s2p($^3$P)3s | $^4$P $^o_{3/2}$ | 1074631. | 1078000 | 1077762 | 1077755 | 2.762E−11 | 1.681E−11 | 1.692E−11 |
| 21 | 2s2p($^3$P)3s | $^4$P $^o_{5/2}$ | 1075911. | 1079330 | 1079074 | 1079036 | 2.772E−11 | 1.674E−11 | 1.678E−11 |
| 22 * | 2s $^2$3d | $^2$D $_{3/2}$ | 1081549. | 1060580 | 1060482 | 1060463 | 3.343E−12 | 3.782E−12 | 3.778E−12 |
| 23 | 2s $^2$3d | $^2$D $_{5/2}$ | 1081705. | 1060700 | 1060612 | 1060592 | 3.354E−12 | 3.793E−12 | 3.793E−12 |
| 24 | 2s2p($^3$P)3s | $^2$P $^o_{1/2}$ | 1107474. | 1103220 | 1103068 | 1103087 | 2.215E−11 | 2.249E−11 | 2.258E−11 |
| 25 | 2s2p($^3$P)3s | $^2$P $^o_{3/2}$ | 1108915. | 1104620 | 1104508 | 1104513 | 2.190E−11 | 2.211E−11 | 2.218E−11 |
| 26 * | 2s2p($^3$P)3p | $^4$D $_{1/2}$ | 1123574. | – | 1128784 | 1128823 | 1.140E−09 | 1.042E−10 | 8.522E−11 |
| 27 | 2s2p($^3$P)3p | $^4$D $_{3/2}$ | 1124068. | – | 1129158 | 1129197 | 1.831E−09 | 1.500E−10 | 1.543E−10 |
| 28 | 2s2p($^3$P)3p | $^4$D $_{5/2}$ | 1124880. | – | 1129813 | 1129855 | 4.550E−09 | 4.708E−09 | 4.425E−09 |
| 29 | 2s2p($^3$P)3p | $^4$D $_{7/2}$ | 1125993. | – | 1130955 | 1130933 | 4.569E−09 | 4.682E−09 | 1.426E−07 |
| 30 * | 2s2p($^3$P)3p | $^2$P $_{1/2}$ | 1130928. | 1126810 | 1126639 | 1126672 | 1.182E−11 | 1.120E−11 | 1.145E−11 |
| 31 | 2s2p($^3$P)3p | $^2$P $_{3/2}$ | 1131222. | 1127430 | 1127284 | 1127330 | 1.301E−11 | 1.094E−11 | 1.089E−11 |
| 32 | 2s2p($^3$P)3p | $^4$S $_{3/2}$ | 1133377. | – | 1140057 | 1140089 | 1.281E−10 | 1.689E−09 | 1.619E−09 |
| 33 | 2s2p($^3$P)3p | $^4$P $_{1/2}$ | 1145469. | – | 1147812 | 1147867 | 1.451E−09 | 1.389E−09 | 1.382E−09 |
| 34 | 2s2p($^3$P)3p | $^4$P $_{3/2}$ | 1145988. | – | 1148361 | 1148413 | 1.485E−09 | 1.372E−09 | 1.364E−09 |
| 35 | 2s2p($^3$P)3p | $^4$P $_{5/2}$ | 1146726. | – | 1149037 | 1149084 | 1.286E−09 | 1.020E−09 | 1.091E−09 |
| 36 | 2s2p($^3$P)3p | $^2$D $_{3/2}$ | 1156419. | 1154780 | 1154694 | 1154774 | 9.707E−12 | 9.812E−12 | 9.802E−12 |
| 37 | 2s2p($^3$P)3p | $^2$D $_{5/2}$ | 1157737. | 1156180 | 1156079 | 1156142 | 9.677E−12 | 9.833E−12 | 9.809E−12 |
| 38 | 2s2p($^3$P)3p | $^2$S $_{1/2}$ | 1174037. | 1172340 | 1172268 | 1172334 | 8.178E−12 | 9.622E−12 | 9.611E−12 |
| 39 | 2s2p($^1$P)3s | $^2$P $^o_{1/2}$ | 1212639. | 1198290 | 1198244 | 1198340 | 1.957E−11 | 1.062E−11 | 1.067E−11 |
| 40 | 2s2p($^1$P)3s | $^2$P $^o_{3/2}$ | 1212762. | 1198290 | 1198282 | 1198372 | 1.983E−11 | 1.046E−11 | 3.980E−11 |
| 41 | 2s2p($^1$P)3p | $^2$D $_{3/2}$ | 1265078. | 1251670 | 1251929 | 1252070 | 8.401E−11 | 6.156E−11 | 8.552E−11 |
| 42 | 2s2p($^1$P)3p | $^2$D $_{5/2}$ | 1265315. | 1252010 | 1252084 | 1252215 | 8.219E−11 | 6.131E−11 | 5.133E−09 |
| 43 | 2s2p($^1$P)3p | $^2$P $_{1/2}$ | 1268598. | 1253350 | 1253401 | 1253544 | 1.690E−11 | 1.957E−11 | 3.830E−11 |
| 44 | 2s2p($^1$P)3p | $^2$P $_{3/2}$ | 1269044. | 1253780 | 1253800 | 1253937 | 1.677E−11 | 1.957E−11 | 1.212E−10 |
| 45 | 2s2p($^1$P)3p | $^2$S $_{1/2}$ | 1284069. | 1258880 | 1258410 | 1259323 | 5.128E−11 | 1.963E−11 | 5.661E−11 |

The radiative data (radiative decay rates, oscillator strengths and line strengths) are presented in Table 3 and compared to the RCI Jönsson *et al.* [11], to the MCHF [10] and to the NIST [44] results. We remark that the agreements are better for transitions involving lower levels ($i \leq 16$) than those involving higher levels.

**Table 3:** Present Na VII radiative decay rates ($A_{ij}$) and weighted oscillator strengths ($gf$) including the first 20 levels compared to the RCI results [11] and to the MCHF ones [10]. Transitions with $A_{ij}$ above $10^6$ s $^{-1}$ are presented.

| | | $A_{ij}$ (s$^{-1}$) | | | $gf$ | | S | |
|---|---|---|---|---|---|---|---|---|
| Trans. | Present | RCI | NIST | Present | RCI | NIST | Present | MCHF |
| 6 −1 | 1.331E+09 | 1.193E+09 | 1.170E+09 | 1.794E−01 | 1.694E−01 | 1.667E−01 | 0.28011 | 0.27100 |
| 6 −2 | 2.325E+08 | 2.065E+08 | 2.040E+08 | 3.202E−02 | 2.994E−02 | 2.951E−02 | 0.05051 | 0.04816 |
| 7 −2 | 1.516E+09 | 1.354E+09 | 1.330E+09 | 3.130E−01 | 2.946E−01 | 2.904E−01 | 0.49371 | 0.47690 |
| 8 −1 | 2.961E+09 | 2.542E+09 | 2.520E+09 | 1.226E−01 | 1.089E−01 | 1.079E−01 | 0.15005 | 0.13560 |
| 8 −2 | 4.714E+09 | 3.638E+09 | 3.700E+09 | 1.985E−01 | 1.584E−01 | 1.611E−01 | 0.24485 | 0.19830 |
| 9 −1 | 8.878E+09 | 7.499E+09 | 7.410E+09 | 3.003E−01 | 2.787E−01 | 2.761E−01 | 0.33197 | 0.32290 |
| 9 −2 | 5.047E+09 | 4.470E+09 | 4.230E+09 | 1.732E−01 | 1.687E−01 | 1.596E−01 | 0.19296 | 0.19750 |
| 10 −1 | 2.315E+09 | 1.986E+09 | 2.030E+09 | 1.550E−01 | 1.463E−01 | 1.496E−01 | 0.17058 | 0.16880 |
| 10 −2 | 1.169E+10 | 1.005E+10 | 9.880E+09 | 7.943E−01 | 7.512E−01 | 7.396E−01 | 0.88036 | 0.87270 |
| 10 −3 | 2.052E+09 | 1.829E+09 | 1.840E+09 | 1.871E−01 | 1.722E−01 | 1.734E−01 | 0.24015 | 0.22430 |
| 11 −4 | 4.067E+09 | 3.624E+09 | 3.640E+09 | 3.730E−01 | 3.432E−01 | 3.451E−01 | 0.48026 | 0.44850 |
| 11 −5 | 6.010E+09 | 5.359E+09 | 5.390E+09 | 5.568E−01 | 5.119E−01 | 5.152E−01 | 0.72042 | 0.67260 |
| 12 −6 | 3.087E+09 | 2.509E+09 | 2.710E+09 | 4.072E−01 | 3.512E−01 | 5.689E−01 | 0.62865 | 0.55820 |
| 12 −7 | 4.170E+08 | 3.360E+08 | 2.100E+08 | 5.502E−02 | 4.703E−02 | 4.436E−02 | 0.08495 | 0.07473 |
| 12 −9 | 6.325E+08 | 5.543E+08 | 6.170E+08 | 2.375E−01 | 2.014E−01 | 3.436E−01 | 0.61884 | 0.51590 |
| 12 −10 | 1.041E+08 | 9.337E+07 | 9.290E+07 | 4.002E−02 | 3.463E−02 | 3.715E−02 | 0.10550 | 0.08962 |
| 13 −6 | 2.563E+08 | 2.091E+08 | 3.380E+08 | 5.068E−02 | 4.396E−02 | 4.732E−02 | 0.07823 | 0.06980 |
| 13 −7 | 3.298E+09 | 2.677E+09 | 2.500E+09 | 6.523E−01 | 5.624E−01 | 3.556E−01 | 1.00694 | 0.89420 |
| 13 −10 | 7.074E+08 | 6.224E+08 | 6.170E+08 | 4.077E−01 | 3.468E−01 | 3.436E−01 | 1.07422 | 0.89800 |
| 14 −6 | 6.252E+09 | 5.026E+09 | 5.060E+09 | 2.611E−01 | 2.235E−01 | 2.254E−01 | 0.32074 | 0.28310 |
| 14 −8 | 8.870E+08 | 6.846E+08 | 6.920E+08 | 6.043E−02 | 5.097E−02 | 5.164E−02 | 0.09483 | 0.08324 |
| 14 −9 | 2.392E+09 | 2.005E+09 | 2.010E+09 | 2.187E−01 | 1.831E−01 | 1.832E−01 | 0.39759 | 0.33260 |
| 14 −10 | 1.085E+09 | 8.901E+08 | 8.970E+08 | 1.009E−01 | 8.247E−02 | 8.318E−02 | 0.18485 | 0.15080 |
| 15−6 | 6.843E+08 | 5.459E+08 | 5.470E+08 | 5.708E−02 | 4.851E−02 | 4.875E−02 | 0.07009 | 0.06133 |
| 15−7 | 5.422E+09 | 4.356E+09 | 4.390E+09 | 4.524E−01 | 3.869E−01 | 3.908E−01 | 0.55558 | 0.48990 |
| 15 −8 | 1.124E+09 | 9.413E+08 | 9.310E+08 | 1.529E−01 | 1.400E−01 | 1.387E−01 | 0.23983 | 0.22950 |
| 15 −9 | 4.638E+08 | 3.602E+08 | 3.700E+08 | 8.467E−02 | 6.571E−02 | 6.761E−02 | 0.15379 | 0.11920 |
| 15 −10 | 2.878E+09 | 2.366E+09 | 2.380E+09 | 5.341E−01 | 4.380E−01 | 4.395E−01 | 0.97817 | 0.80050 |
| 16−1 | 1.641E+10 | 1.639E+10 | 1.640E+10 | 5.250E−02 | 5.433E−02 | 5.420E−02 | 0.01786 | 0.01878 |
| 16 −2 | 3.318E+10 | 3.301E+10 | 3.290E+10 | 1.066E−01 | 1.099E−01 | 1.096E−01 | 0.03635 | 0.03803 |
| 17 −6 | 8.274E+09 | 3.609E+09 | – | 3.720E−02 | 1.681E−02 | – | 0.01499 | – |
| 17 −16 | 2.734E+08 | 2.554E+08 | – | 2.313E−01 | 2.390E−01 | – | 1.27902 | – |
| 18 −6 | 8.382E+08 | 3.541E+08 | – | 7.528E−03 | 3.294E−03 | – | 0.00303 | – |
| 18 −7 | 7.494E+09 | 3.213E+09 | – | 6.730E−02 | 2.989E−02 | – | 0.02712 | – |
| 18−16 | 2.797E+08 | 2.631E+08 | – | 4.656E−01 | 4.829E−01 | – | 2.55328 | – |
| 19 −3 | 6.025E+09 | 9.923E+09 | – | 1.942E−02 | 3.214E−02 | – | 0.00663 | – |
| 19 −4 | 3.024E+10 | 4.944E+10 | – | 9.766E−02 | 1.604E−01 | – | 0.03337 | – |
| 20 −3 | 1.500E+10 | 2.482E+10 | – | 9.656E−02 | 1.605E−01 | – | 0.03294 | – |
| 20 −4 | 4.818E+09 | 7.879E+09 | 7.910E+09 | 3.106E−02 | 5.103E−02 | 5.117E−02 | 0.01061 | 0.01752 |
| 20 −5 | 1.638E+10 | 2.678E+10 | 2.670E+10 | 1.059E−01 | 1.738E−01 | 1.734E−01 | 0.03619 | 0.05929 |

We recapitulate the results of the comparisons in the Table 4, where the three first columns are for the relative errors for the radiative decay rates and the second last ones for oscillator strengths and line strengths:

**Table 4:** Averaged relative errors for Ar VII radiative data

| Method→ | RCI | MCHF | NIST | RCI | MCHF |
|---|---|---|---|---|---|
| $i-j\downarrow$ | | | | | |
| $i \leq 16$ | 15 | 14 | 16 | 11 | 11 |
| $i \geq 17$ | 38 | 56 | 28 | 38 | 55 |
| All | 25 | 28 | 19 | 23 | 25 |

where it is shown that for transitions $i-j$ for which $1 \leq i \leq 16$, the relative error between our results and the three approaches is about 15 % for the radiative decay rates and 10 % for the oscillator strengths and line strengths. The agreement becomes less for transitions involving the levels 20 and higher and the relative error (averaged over the the results of the three approaches) reaches 40 %. These levels arise from the configuration 2s2p3s. If we take into account all the transitions presented in Table 3, the averaged agreement is between 20 % and 25 %. In the line broadening calculations (next subsection), we will not consider transitions involving levels arising from the 2s2p3s configuration.

**Table 5:** Our energy levels ($E$) in cm $^{-1}$ for Na VIII compared to NIST [44], to the MCHF [10] and to the Many–Body Perturbation Theory (MBPT) approach [12]. Our lifetimes $\tau$ are compared to the MCHF [10] and to the MBPT approach [12] .

| Index | Conf. | Level | $E$ | NIST | MCHF | MBPT | $\tau$(s) | $\tau_{MCHF}$(s) | $\tau_{MBPT}$(s) |
|---|---|---|---|---|---|---|---|---|---|
| 1 | 2s $^2$ | $^1$S $_0$ | 0 | 0 | 0 | 0 | – | – | – |
| 2 | 2s2p | $^3$P $^o_0$ | 126620. | 125881 | 126238.01 | 125738.9 | – | – | – |
| 3 | 2s2p | $^3$P $^o_1$ | 127452. | 126613 | 126974.98 | 126467.2 | – | 2.183E−05 | 2.220E−05 |
| 4 | 2s2p | $^3$P $^o_2$ | 129149. | 128219 | 128587.82 | 128079.3 | – | 6.934E+00 | 7.007E+00 |
| 5 | 2s2p | $^1$P $^o_1$ | 252488. | 243208 | 243705.76 | 242685.8 | 1.976E−10 | 2.182E−10 | 2.208E−10 |
| 6 | 2p $^2$ | $^3$P $_0$ | 331049. | – | 328617.11 | 326963.4 | 2.700E−10 | 2.803E−10 | 2.847E−10 |
| 7 | 2p $^2$ | $^3$P $_1$ | 331927. | – | 329462.71 | 327806.9 | 2.682E−10 | 2.785E−10 | 2.828E−10 |
| 8 | 2p $^2$ | $^3$P $_2$ | 333567. | – | 330889.08 | 329220.8 | 2.652E−10 | 2.760E−10 | 2.803E−10 |
| 9 | 2p $^2$ | $^1$D $_2$ | 369898. | – | 362430.49 | 360243.3 | 1.485E−09 | 1.457E−09 | 1.501E−09 |
| 10 | 2p $^2$ | $^1$S $_0$ | 460409. | – | 447544.50 | 444922.2 | 1.347E−10 | 1.496E−10 | 1.536E−10 |
| 11 | 2s3s | $^3$S $_1$ | 1238299. | 1239975 | 1240797.27 | 1238642. | 1.121E−11 | 1.135E−11 | 1.145E−11 |
| 12 | 2s3s | $^1$S $_0$ | 1262669. | 1262780 | 1263577.94 | 1261224. | 2.831E−11 | 3.546E−11 | 3.633E−11 |
| 13 | 2s3p | $^1$P $^o_1$ | 1294165. | 1294230 | 1294894.64 | 1292685. | 4.900E−12 | 4.936E−12 | 4.958E−12 |
| 14 | 2s3p | $^3$P $^o_0$ | 1296268. | – | 1297815.73 | 1295730. | 1.010E−09 | 1.099E−09 | 1.040E−09 |
| 15 | 2s3p | $^3$P $^o_1$ | 1296531. | – | 1298043.91 | 1295948. | 2.454E−10 | 3.951E−10 | 4.139E−10 |
| 16 | 2s3p | $^3$P $^o_2$ | 1296949. | – | 1298451.81 | 1296359. | 9.598E−10 | 1.034E−09 | 1.002E−09 |
| 17 | 2s3d | $^3$D $_1$ | 1327318. | 1327230 | 1327885.95 | 1325741. | 2.516E−12 | 2.506E−12 | 2.511E−12 |
| 18 | 2s3d | $^3$D $_2$ | 1327413. | 1327270 | 1327955.68 | 1325797. | 2.519E−12 | 2.510E−12 | 2.515E−12 |
| 19 | 2s3d | $^3$D $_3$ | 1327554. | 1327390 | 1328078.04 | 1325934. | 2.524E−12 | 2.516E−12 | 2.521E−12 |
| 20 | 2s3d | $^1$D $_2$ | 1351487. | 1347740 | 1348420.34 | 1345802. | 3.827E−12 | 3.881E−12 | 3.889E−12 |

**Table 6:** Contionued. Levels marked by (+) are evaluated by NIST as "may be not real".

| Index | Conf. | Level | $E$ | NIST | MBPT | $\tau$(s) | $\tau_{MBPT}$(s) |
|---|---|---|---|---|---|---|---|
| 21 | 2p3s | $^3$P $^o_0$ | 1400160. | 1399670 | 1398104. | 1.397E−11 | 1.521E−11 |
| 22 | 2p3s | $^3$P $^o_1$ | 1400945. | 1400470 | 1398878. | 1.391E−11 | 1.513E−11 |
| 23 | 2p3s | $^3$P $^o_2$ | 1402650. | 1402200 | 1400618. | 1.381E−11 | 1.497E−11 |
| 24 | 2p3s | $^1$P $^o_1$ | 1427627. | 1426120 | 1419970. | 1.134E−11 | 1.265E−11 |
| 25 | 2p3p | $^1$P $_1$ | 1432513. | 1432980 | 1431483. | 7.724E−12 | 9.352E−12 |
| 26 $^+$ | 2p3p | $^3$D $_1$ | 1439628. | 1439410 | 1437839. | 1.793E−11 | 1.840E−11 |
| 27 $^+$ | 2p3p | $^3$D $_2$ | 1440531. | 1440260 | 1438717. | 1.830E−11 | 1.875E−11 |
| 28 | 2p3p | $^3$D $_3$ | 1442138. | 1441880 | 1440337. | 1.816E−11 | 1.865E−11 |
| 29 | 2p3p | $^3$S $_1$ | 1452834. | 1452400 | 1450786. | 9.445E−12 | 1.092E−11 |
| 30 | 2p3p | $^3$P $_0$ | 1461251. | – | 1457417. | 1.061E−11 | 1.070E−11 |
| 31 | 2p3p | $^3$P $_1$ | 1461907. | 1459850 | 1458101. | 1.061E−11 | 1.070E−11 |
| 32 | 2p3p | $^3$P $_2$ | 1462915. | 1460770 | 1459004. | 1.062E−11 | 1.070E−11 |
| 33 | 2p3d | $^3$F $^o_2$ | 1467581. | – | 1464643. | 1.591E−11 | 6.163E−11 |
| 34 | 2p3d | $^3$F $^o_3$ | 1469108. | – | 1465771. | 6.569E−10 | 7.368E−10 |
| 35 | 2p3d | $^1$D $^o_2$ | 1469334. | 1469150 | 1467028. | 8.991E−12 | 5.040E−09 |
| 36 | 2p3d | $^3$F $^o_4$ | 1470388. | – | 1467568. | 3.202E−09 | 6.430E−12 |
| 37 | 2p3p | $^1$D $_2$ | 1481106. | 1474580 | 1472273. | 6.571E−12 | 7.435E−12 |
| 38 | 2p3d | $^3$D $^o_1$ | 1485631. | 1485140 | 1483407. | 2.004E−12 | 2.089E−12 |
| 39 | 2p3d | $^3$D $^o_2$ | 1485978. | 1485340 | 1483761. | 2.016E−12 | 2.103E−12 |
| 40 | 2p3d | $^3$D $^o_3$ | 1486609. | 1486080 | 1484382. | 1.999E−12 | 2.083E−12 |
| 41 | 2p3d | $^3$P $^o_2$ | 1492779. | 1491980 | 1490287. | 3.703E−12 | 3.874E−12 |
| 42 | 2p3d | $^3$P $^o_1$ | 1493372. | 1492630 | 1490932. | 3.721E−12 | 3.892E−12 |
| 43 | 2p3d | $^3$P $^o_0$ | 1493670. | 1492980 | 1491286. | 3.744E−12 | 3.921E−12 |
| 44 | 2p3p | $^1$S $_0$ | 1511981. | 1481510 | 1497353. | 1.834E−11 | 1.487E−11 |
| 45 | 2p3d | $^1$F $^o_3$ | 1516888. | 1507790 | 1505345. | 1.586E−12 | 1.776E−12 |
| 46 | 2p3d | $^1$P $^o_1$ | 1519737. | 1513730 | 1511315. | 2.630E−12 | 3.086E−12 |
| 47 | 2p4s | $^3$S $^o_1$ | 1649675. | 1649480 | 1647631. | 2.688E−11 | 2.561E−11 |
| 48 | 2p4s | $^1$S $^o_0$ | 1662154. | 1656820 | 1656380. | 2.285E−11 | 3.161E−11 |
| 49 | 2s4p | $^3$P $^o_0$ | 1671030. | – | 1669537. | 7.975E−11 | 7.487E−11 |
| 50 | 2s4p | $^3$P $^o_1$ | 1671120. | – | 1669609. | 7.936E−11 | 7.213E−11 |
| 51 | 2s4p | $^3$P $^o_2$ | 1671311. | – | 1669794. | 8.031E−11 | 7.547E−11 |
| 52 | 2s4p | $^1$P $^o_1$ | 1675965. | 1673390 | 1671261. | 8.202E−12 | 9.696E−12 |
| 53 | 2s4d | $^3$D $_1$ | 1682870. | 1683370 | 1681339. | 6.558E−12 | 6.387E−12 |
| 54 | 2s4d | $^3$D $_2$ | 1682900. | 1683370 | 1681364. | 6.554E−12 | 6.393E−12 |
| 55 | 2s4d | $^3$D $_3$ | 1682945. | 1683370 | 1681412. | 6.547E−12 | 6.403E−12 |
| 56 | 2s4d | $^1$D $_2$ | 1690982. | 1689970 | 1687841. | 6.389E−12 | 8.217E−12 |

**Table 7:** Present Na VIII radiative decay rates ($A_{ij}$) and oscillator strengths ($gf$) compared to the NIST [44] values taken from Kelleher & Podobedova [48], and to the MBPT results [12]. Only transitions with decay rates above $10^6$ s$^{-1}$ are presented.

| | | $A_{ij}$ (s$^{-1}$) | | | $gf$ | | S | |
|---|---|---|---|---|---|---|---|---|
| Trans. | Present | NIST | MBPT | Present | NIST | MBPT | Present | MBPT |
| 5 −1 | 5.060E+09 | 4.400E+09 | 4.528E+09 | 3.570E−01 | 3.350E−01 | 3.450E−01 | 0.46549 | 0.46750 |
| 6 −3 | 3.704E+09 | 3.510E+09 | 3.512E+09 | 1.340E−01 | 1.305E−01 | 1.307E−01 | 0.21660 | 0.21440 |
| 7 −2 | 1.267E+09 | 1.200E+09 | 1.200E+09 | 1.352E−01 | 1.320E−01 | 1.319E−01 | 0.21675 | 0.21470 |
| 7 −3 | 9.382E+08 | 8.890E+08 | 8.899E+08 | 1.009E−01 | 9.840E−02 | 9.852E−02 | 0.16249 | 0.16090 |
| 7 −4 | 1.524E+09 | 1.450E+09 | 1.445E+09 | 1.667E−01 | 1.625E−01 | 1.626E−01 | 0.27058 | 0.26770 |
| 8 −3 | 9.617E+08 | 9.090E+08 | 9.099E+08 | 1.697E−01 | 1.653E−01 | 1.655E−01 | 0.27103 | 0.26850 |
| 8−4 | 2.809E+09 | 2.660E+09 | 2.657E+09 | 5.039E−01 | 4.905E−01 | 4.913E−01 | 0.81152 | 0.80320 |
| 8 −5 | 6.681E+08 | 6.660E+08 | 6.599E+08 | 3.633E−01 | 3.600E−01 | 3.570E−01 | 1.01866 | 0.99900 |
| 10 −5 | 7.425E+09 | 6.590E+09 | 6.510E+09 | 2.575E−01 | 2.400E−01 | 2.381E−01 | 0.44772 | 0.38720 |
| 11 −2 | 9.863E+09 | 9.930E+09 | 9.679E+09 | 3.590E−02 | 3.600E−02 | 3.507E−02 | 0.01063 | 0.01036 |
| 11−3 | 2.966E+10 | 2.980E+10 | 2.908E+10 | 1.081E−01 | 1.083E−01 | 1.055E−01 | 0.03204 | 0.03120 |
| 11−4 | 4.967E+10 | 4.980E+10 | 4.858E+10 | 1.816E−01 | 1.815E−01 | 1.768E−01 | 0.05390 | 0.05234 |
| 12 −5 | 3.533E+10 | 2.980E+10 | 2.753E+10 | 5.190E−02 | 4.290E−02 | 3.969E−02 | 0.01692 | 0.01281 |
| 13 −1 | 1.889E+11 | 1.870E+11 | 1.911E+11 | 5.074E−01 | 5.020E−01 | 5.132E−01 | 0.12907 | 0.13060 |
| 13 −9 | 1.467E+11 | 1.170E+11 | 1.007E+10 | 7.726E−02 | 6.050E−02 | 5.195E−02 | 0.02752 | 0.01830 |
| 13 −12 | 3.001E+07 | 3.100E+07 | 3.092E+07 | 1.361E−01 | 1.410E−01 | 1.403E−01 | 1.42226 | 1.46600 |
| 14 −11 | 2.492E+08 | – | 2.370E+08 | 1.112E−01 | – | 1.088E−01 | 0.63150 | 0.62670 |
| 15−6 | 2.566E+08 | – | 2.443E+08 | 1.238E−03 | – | 1.168E−03 | 0.00042 | 0.00040 |
| 15−7 | 1.800E+08 | – | 1.736E+08 | 8.700E−04 | – | 8.310E−04 | 0.00030 | 0.00028 |
| 15 −8 | 2.875E+08 | – | 2.828E+08 | 1.394E−03 | – | 1.358E−03 | 0.00048 | 0.00046 |
| 15 −11 | 2.488E+08 | – | 2.381E+08 | 3.300E−01 | – | 3.252E−01 | 1.86577 | 1.86700 |
| 16−7 | 2.057E+08 | – | 1.917E+08 | 1.656E−03 | – | 1.529E−03 | 0.00057 | 0.00052 |
| 16 −8 | 5.775E+08 | – | 5.479E+08 | 4.665E−03 | – | 4.382E−03 | 0.00159 | 0.00149 |
| 16 −11 | 2.583E+08 | – | 2.453E+08 | 5.630E−01 | – | 5.508E−01 | 3.15998 | 3.13800 |
| 17−2 | 2.209E+11 | 2.230E+11 | 2.214E+11 | 6.893E−01 | 6.940E−01 | 6.898E−01 | 0.18899 | 0.18900 |
| 17−3 | 1.655E+11 | 1.670E+11 | 1.658E+11 | 5.171E−01 | 5.220E−01 | 5.175E−01 | 0.14189 | 0.14190 |
| 17 − 4 | 1.101E+10 | 1.110E+11 | 1.104E+10 | 3.451E−02 | 3.475E−02 | 3.453E−02 | 0.00948 | 0.00948 |
| 18 −3 | 2.978E+11 | 3.000E+11 | 2.983E+11 | 1.551E+00 | 1.560E+00 | 1.551E+00 | 0.42541 | 0.42530 |
| 18−4 | 9.909E+10 | 9.990E+10 | 9.924E+10 | 5.173E−01 | 5.200E−01 | 5.175E−01 | 0.14213 | 0.14210 |
| 19 −4 | 3.961E+11 | 3.990E+11 | 3.966E+11 | 2.895E+00 | 2.915E+00 | 2.895E+00 | 0.79518 | 0.79460 |
| 19 −16 | 2.893E+07 | – | 2.611E+07 | 3.242E−01 | – | 3.126E−01 | 3.48731 | 3.47600 |
| 20 − 5 | 2.611E+11 | 2.540E+11 | 2.569E+11 | 1.621E+00 | 1.563E+00 | 1.579E+00 | 0.48546 | 0.47070 |
| 20−13 | 1.946E+08 | 1.630E+08 | 1.588E+08 | 4.439E−01 | 4.260E−01 | 4.209E−01 | 2.54941 | 2.60600 |
| 21 −7 | 7.079E+10 | 6.920E+10 | 6.502E+10 | 9.300E−02 | 9.030E−02 | 8.490E−02 | 0.02866 | 0.02608 |
| 21 −11 | 7.815E+08 | 7.500E+08 | 7.346E+08 | 4.472E−02 | 4.410E−02 | 4.320E−02 | 0.09097 | 0.08911 |
| 21 −17 | 1.505E+07 | 1.040E+07 | 9.513E+06 | 4.251E−03 | 2.979E−03 | 2.718E−03 | 0.01921 | 0.01235 |
| 22−6 | 2.369E+10 | 2.330E+10 | 2.185E+10 | 9.309E−02 | 9.090E−02 | 8.534E−02 | 0.02864 | 0.02618 |
| 22−7 | 1.759E+10 | 1.720E+10 | 1.615E+10 | 6.921E−02 | 6.750E−02 | 6.318E−02 | 0.02132 | 0.01940 |
| 22 −8 | 2.973E+10 | 2.900E+10 | 2.725E+10 | 1.174E−01 | 1.135E−01 | 1.069E−01 | 0.03620 | 0.03286 |
| 22 −11 | 7.907E+08 | 7.610E+08 | 7.434E+08 | 1.344E−01 | 1.329E−01 | 1.299E−01 | 0.27213 | 0.26660 |

For the Na VIII ion, we have used 12 configurations: 1s $^2$ [2s $^2$, 2s2p, 2s3s, 2s3p, 2s3d, 2p3s, 2p3p, 2p3d, 2s4s, 2s4p, 2s4d]. The energy levels are presented in Tables 5 and 6, and compared with NIST [44], with the MCHF [10], with the Relativistic Many–Body [18] results (RMB) and with the Many–Body Perturbation Theory (MBPT) approach [12]. Lifetimes are compared with the MCHF results [10] and with the MBPT ones [12]. The energies agree well with all the other results within 2 %. Our radiative data for Na VIII are presented in Table 7 and they agree better with the other results than those of Na VII. The relative difference is about 8 % for the radiative decay rates and 6 % for the oscillator strengths and line strengths.

Collision strengths in intermediate coupling (between fine structure levels) have been also calculated. We have included in JAJOM partial partial wave of the scattered electron $l$ up to 29. For high $l$, the collision strengths of allowed transitions have been calculated using the Coulomb–Bethe formulation [49] and for forbidden transitions, it is assumed that collision strengths follow geometric series behaviour with partial wave [50,51]. We present some of our collision strengths in Tables 8 and 9 with the relativistic distorted wave calculations [20] for Na VII and in Tables 10 and 11 some of the Na VIII collision strengths with the relativistic distorted wave calculations [21]. For each ion we divide the results of the collision strengths in two tables depending on whether the values are high ($\Omega > 1$) or low ($\Omega < 1$). This is will be discussed in details in the second paragraph. The calculations have been performed at four incident electron energies; we use the same energies (displayed in Tables 7−10) as in Zhang & Sampson (1992, 1994)[20,21] to perform the comparisons. Zhang & Sampson (1992, 1994) [20,21] included in their work three configurations for each ion: 1s $^2$2s $^2$2p, 1s $^2$2s2p $^2$, 1s $^2$2p $^3$ for Na VII and 1s $^2$2s $^2$, 1s $^2$2s2p, 1s $^2$2p $^2$ for Na VIII. We present also in these tables the relative errors for each transition at each energy.

Even though the averaged agreement –over all the transitions– between our results and those of Zhang & Sampson (1992, 1994) [20,21] is acceptable (11 % for Na VII and 18 for Na VIII), there are some details that have to be discussed. In fact, we note that the behaviour of this agreement for transitions with low collision strengths ($\Omega < 1$) is different from that of transitions with high collision strengths ($\Omega > 1$). So, we divide the two Tables 4 and 5 in two groups of transitions: the first group with low collision strengths ($\Omega < 1$) and the second one with high collision strengths ($\Omega > 1$). This remark and the following discussions are applicable for the two ions. The first group presents an excellent agreement: 5 % with Zhang & Sampson (1994) [20] for Na VII and 11 % with Zhang & Sampson (1992)[21] for Na VIII. Furthermore, the difference between the two results –for almost all transitions of this group– is decreasing with the electron energy (from 10 % to 5 % for Na VII and from 20 % to 8 % for Na VIII). For the second group of transitions, the agreement is worse and the difference is increasing with energy: for Na VII, it increases from 8 % to 56 % with an average of 28 %, and for Na VIII, it increases from 8 % to 79 % with an average of 39 %. Since this behaviour depends on electron energy, and in order to investigate its potential origin, we select two transitions of each ion and for illustration, we

**Table 8:** Present Na VII collision strengths at four electron energies $\varepsilon$ in Ryd compared to the relativistic distorted wave calculations (ZS94) of Zhang & Sampson (1994). $E_{ij}$ is the energy difference of the transition, $\Delta = 100 \times \frac{|\text{Present}-\text{ZS94}|}{\text{ZS94}}$ (%) and "**Avg.**" is the average of Δ values in a column.

| Trans. | $\varepsilon_1 = E_{ij} + 11.77$ | | | $\varepsilon_2 = E_{ij} + 24.71$ | | | $\varepsilon_3 = E_{ij} + 47.06$ | | | $\varepsilon_4 = E_{ij} + 82.36$ | | |
|---|---|---|---|---|---|---|---|---|---|---|---|---|
| $i-j$ | Present | ZS94 | Δ | Present | ZS94 | Δ | Present | ZS94 | Δ | Present | ZS94 | Δ |
| 1 −2 | 1.81E−01 | 1.80E−01 | 1 | 1.37E−01 | 1.40E−01 | 2 | 1.20E−01 | 1.24E−01 | 3 | 1.14E−01 | 1.20E−01 | 5 |
| 1 −3 | 1.82E−02 | 1.73E−02 | 5 | 8.96E−03 | 9.13E−03 | 2 | 4.00E−03 | 4.18E−03 | 5 | 1.84E−03 | 1.90E−03 | 3 |
| 1 −4 | 2.62E−02 | 2.48E−02 | 5 | 1.28E−02 | 1.30E−02 | 2 | 5.59E−03 | 5.82E−03 | 4 | 2.42E−03 | 2.51E−03 | 4 |
| 1 −5 | 1.52E−02 | 1.43E−02 | 6 | 7.51E−03 | 7.38E−03 | 2 | 3.23E−03 | 3.36E−03 | 4 | 1.40E−03 | 1.45E−03 | 4 |
| 1 −7 | 2.91E−02 | 2.69E−02 | 8 | 1.44E−02 | 1.41E−02 | 2 | 6.34E−03 | 6.35E−03 | 0 | 2.76E−03 | 2.74E−03 | 1 |
| 1−12 | 5.45E−03 | 5.69E−03 | 4 | 6.44E−03 | 6.60E−03 | 2 | 7.21E−03 | 7.41E−03 | 3 | 7.61E−03 | 7.96E−03 | 5 |
| 1 −13 | 4.15E−03 | 4.39E−03 | 6 | 4.37E−03 | 4.53E−03 | 4 | 4.64E−03 | 4.83E−03 | 4 | 4.81E−03 | 5.09E−03 | 6 |
| 1 −15 | 2.84E−03 | 3.05E−03 | 7 | 3.10E−03 | 3.28E−03 | 6 | 3.38E−03 | 3.58E−03 | 6 | 3.55E−03 | 3.82E−03 | 8 |
| 2−3 | 1.14E−02 | 1.08E−02 | 5 | 5.62E−03 | 5.75E−03 | 2 | 2.53E−03 | 2.67E−03 | 6 | 1.16E−03 | 1.26E−03 | 9 |
| 2 −4 | 3.27E−02 | 3.09E−02 | 6 | 1.59E−02 | 1.62E−02 | 2 | 7.01E−03 | 7.29E−03 | 4 | 3.06E−03 | 3.18E−03 | 4 |
| 2 −5 | 7.32E−02 | 6.94E−02 | 5 | 3.58E−02 | 3.66E−02 | 2 | 1.58E−02 | 1.65E−02 | 4 | 6.96E−03 | 7.35E−03 | 6 |
| 2 −6 | 2.87E−01 | 3.10E−01 | 8 | 2.85E−01 | 3.43E−01 | 20 | 2.65E−01 | 3.84E−01 | 45 | 3.21E−01 | 4.26E−01 | 33 |
| 2 −11 | 1.45E−03 | 1.84E−03 | 27 | 6.70E−04 | 7.44E−04 | 11 | 2.40E−04 | 2.43E−04 | 1 | 4.80E−05 | 6.35E−05 | 19 |
| 2 −12 | 5.83E−03 | 6.17E−03 | 6 | 6.24E−03 | 6.48E−03 | 4 | 6.71E−03 | 6.98E−03 | 4 | 6.98E−03 | 7.39E−03 | 6 |
| 2 −13 | 1.28E−02 | 1.34E−02 | 5 | 1.46E−02 | 1.51E−02 | 3 | 1.61E−02 | 1.68E−02 | 4 | 1.69E−02 | 1.80E−02 | 7 |
| 2 −14 | 3.08E−03 | 3.28E−03 | 6 | 3.83E−03 | 3.53E−03 | 4 | 3.70E−03 | 3.86E−03 | 4 | 3.88E−03 | 4.12E−03 | 6 |
| 3−4 | 1.37E−01 | 1.25E−01 | 9 | 6.74E−02 | 6.57E−02 | 3 | 3.48E−02 | 3.49E−02 | 0 | 2.14E−02 | 2.19E−02 | 2 |
| 3 −5 | 1.11E−01 | 1.12E−01 | 1 | 1.04E−01 | 1.07E−01 | 3 | 1.04E−01 | 1.08E−01 | 4 | 1.06E−01 | 1.11E−01 | 5 |
| 3 −6 | 5.15E−02 | 4.62E−02 | 10 | 2.15E−02 | 2.07E−02 | 4 | 8.11E−03 | 7.93E−03 | 2 | 3.04E−03 | 2.88E−03 | 5 |
| 3 −7 | 3.08E−02 | 2.74E−02 | 11 | 1.32E−02 | 1.27E−02 | 4 | 5.15E−03 | 5.07E−03 | 2 | 1.99E−03 | 1.96E−03 | 2 |
| 3 −8 | 1.07E−02 | 9.70E−03 | 9 | 3.88E−03 | 3.85E−03 | 1 | 1.26E−03 | 1.21E−03 | 4 | 3.79E−04 | 3.91E−04 | 3 |
| 3 −9 | 3.49E−03 | 2.88E−03 | 17 | 1.39E−03 | 1.30E−03 | 6 | 5.37E−04 | 5.30E−04 | 1 | 2.17E−04 | 2.19E−04 | 1 |
| 3 −10 | 8.06E−03 | 7.07E−03 | 12 | 3.34E−03 | 3.27E−03 | 2 | 1.29E−03 | 1.30E−03 | 1 | 5.01E−04 | 5.04E−04 | 1 |
| 3 −12 | 1.92E−02 | 1.74E−02 | 9 | 9.57E−03 | 9.11E−03 | 5 | 4.14E−03 | 4.09E−03 | 1 | 1.75E−03 | 1.77E−03 | 1 |
| 3 −13 | 2.14E−03 | 1.90E−03 | 11 | 1.04E−03 | 9.90E−04 | 5 | 4.49E−04 | 4.43E−04 | 1 | 1.89E−04 | 1.91E−04 | 1 |
| 3 −14 | 4.97E−03 | 4.36E−03 | 12 | 2.35E−03 | 2.25E−03 | 4 | 1.01E−03 | 1.01E−03 | 0 | 4.41E−04 | 4.57E−04 | 4 |
| 3 −15 | 2.94E−03 | 2.58E−03 | 12 | 1.37E−03 | 1.31E−03 | 4 | 5.77E−04 | 5.73E−04 | 1 | 2.44E−04 | 2.40E−04 | 2 |
| 4−5 | 2.90E−01 | 2.79E−01 | 4 | 2.06E−01 | 2.08E−01 | 1 | 1.71E−01 | 1.76E−01 | 3 | 1.58E−01 | 1.66E−01 | 5 |
| 4 −6 | 8.02E−02 | 7.17E−02 | 11 | 3.36E−02 | 3.22E−02 | 4 | 1.27E−02 | 1.25E−02 | 2 | 4.79E−03 | 4.62E−03 | 4 |
| 4 −7 | 8.47E−02 | 7.60E−02 | 10 | 3.59E−02 | 3.48E−02 | 3 | 1.38E−02 | 1.36E−02 | 1 | 5.26E−03 | 5.19E−03 | 1 |
| 4 −8 | 2.05E−02 | 1.90E−02 | 7 | 7.67E−03 | 7.49E−03 | 2 | 2.48E−03 | 2.40E−03 | 3 | 7.39E−04 | 6.83E−04 | 8 |
| 4 −9 | 7.60E−03 | 6.42E−03 | 16 | 3.08E−03 | 2.91E−03 | 6 | 1.19E−03 | 1.16E−03 | 3 | 4.73E−03 | 4.38E−03 | 7 |
| 4 −10 | 1.62E−02 | 1.40E−02 | 14 | 6.66E−03 | 6.44E−03 | 3 | 2.57E−03 | 2.57E−03 | 0 | 1.00E−03 | 1.01E−03 | 1 |
| 4 −12 | 2.56E−02 | 2.32E−02 | 9 | 1.28E−02 | 1.22E−02 | 5 | 5.60E−03 | 5.58E−03 | 0 | 2.42E−03 | 2.52E−03 | 4 |
| 4 −13 | 1.68E−02 | 1.52E−02 | 10 | 8.36E−03 | 7.98E−03 | 5 | 3.62E−03 | 3.59E−03 | 1 | 1.54E−03 | 1.57E−03 | 2 |
| 4 −14 | 7.48E−03 | 6.53E−03 | 13 | 3.52E−03 | 3.33E−03 | 5 | 1.49E−03 | 1.46E−03 | 2 | 6.31E−04 | 6.13E−04 | 3 |
| 4 −15 | 8.98E−03 | 7.87E−03 | 12 | 4.28E−03 | 4.08E−03 | 5 | 1.88E−03 | 1.86E−03 | 1 | 8.56E−04 | 8.78E−04 | 3 |
| Avg. | | | 10 | | | 4 | | | 3 | | | 5 |

**Table 9:** Continued.

| Trans. | $\varepsilon_1 = E_{ij} + 11.77$ | | | $\varepsilon_2 = E_{ij} + 24.71$ | | | $\varepsilon_3 = E_{ij} + 47.06$ | | | $\varepsilon_4 = E_{ij} + 82.36$ | | |
|---|---|---|---|---|---|---|---|---|---|---|---|---|
| $i-j$ | Present | ZS94 | Δ | Present | ZS94 | Δ | Present | ZS94 | Δ | Present | ZS94 | Δ |
| 1 −6 | 1.38E+00 | 1.52E+00 | 10 | 1.47E+00 | 1.79E+00 | 22 | 1.42E+00 | 2.07E+00 | 46 | 1.30E+00 | 2.32E+00 | 79 |
| 1 −8 | 6.73E−01 | 6.69E−01 | 1 | 7.46E−01 | 7.89E−01 | 6 | 7.44E−01 | 9.13E−01 | 23 | 6.89E−01 | 1.03E+00 | 49 |
| 1 −9 | 1.42E+00 | 1.47E+00 | 4 | 1.61E+00 | 1.75E+00 | 9 | 1.64E+00 | 2.03E+00 | 24 | 1.53E+00 | 2.31E+00 | 51 |
| 1 −10 | 7.35E−01 | 7.58E−01 | 3 | 8.27E−01 | 8.97E−01 | 8 | 8.38E−01 | 1.04E+00 | 24 | 7.83E−01 | 1.18E+00 | 51 |
| 1 −14 | 4.14E−03 | 2.18E−03 | 47 | 4.11E−03 | 2.05E−03 | 50 | 4.02E−03 | 1.98E−03 | 51 | 3.94E−03 | 1.95E−03 | 51 |
| 2−7 | 2.47E+00 | 2.71E+00 | 10 | 2.60E+00 | 3.17E+00 | 22 | 2.49E+00 | 3.66E+00 | 47 | 2.27E+00 | 4.10E+00 | 81 |
| 2 −8 | 1.10E+00 | 1.10E+00 | 0 | 1.22E+00 | 1.30E+00 | 7 | 1.21E+00 | 1.50E+00 | 24 | 1.12E+00 | 1.69E+00 | 51 |
| 2 −9 | 8.37E−01 | 8.58E−01 | 3 | 9.41E−01 | 1.02E+00 | 8 | 9.55E−01 | 1.18E+00 | 24 | 8.92E−01 | 1.34E+00 | 50 |
| 2 −10 | 3.79E+00 | 3.91E+00 | 3 | 4.27E+00 | 4.64E+00 | 9 | 4.34E+00 | 5.38E+00 | 24 | 4.06E+00 | 6.11E+00 | 50 |
| 3−11 | 1.10E+00 | 1.16E+00 | 5 | 1.22E+00 | 1.37E+00 | 12 | 1.21E+00 | 1.58E+00 | 31 | 1.12E+00 | 1.78E+00 | 59 |
| 4−11 | 2.20E+00 | 2.31E+00 | 5 | 2.44E+00 | 2.73E+00 | 12 | 2.42E+00 | 3.16E+00 | 31 | 2.24E+00 | 3.56E+00 | 59 |
| 5−11 | 3.29E+00 | 3.47E+00 | 5 | 3.66E+00 | 4.09E+00 | 11 | 3.64E+00 | 4.73E+00 | 23 | 3.36E+00 | 5.34E+00 | 37 |
| Avg. | | | 8 | | | 15 | | | 31 | | | 56 |

plot their collision strengths as a function of the electron energy. In Fig 1, we plot the Na VII collision strengths for the transitions $2s2p\ ^2{}^2D_{3/2} - 2s\ ^2 2p\ ^2P^o_{1/2}$ (6–1) and $2p^3\ ^4S^o_{3/2} - 2s2p^2\ ^4P_{5/2}$ (5–11), and those of the Na VIII transitions $2s2p\ ^1P^o_1 - 2s^2\ ^1S_0$ (5–1) and $2p^2\ ^3P_2 - 2s2p\ ^3P^o_2$ (8–4). We see that the collision strengths of Zhang & Sampson (1992, 1994)[20,21] do not converge at high energies, in contrast to ours which decrease to converge toward the infinite energy Born limit. This (and the difference in the configurations used in the calculations) maybe the origin of the high disagreement between the two calculations for these transitions.

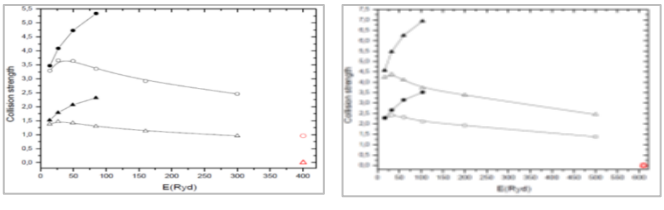


**Figure 1:** Collision strength Ω as a function of the incident electron energy, open symbols are for the present results. Left: the two Na VII transitions: $2s2p\ ^2{}^2D_{3/2} - 2s\ ^2 2p\ ^2P^o_{1/2}$ (△) and $2p^3\ ^4S^o_{3/2} - 2s2p^2\ ^4P_{5/2}$ (∘), solid symbols: results of ZS94. Right: the two Na VIII transitions: $2p^2\ ^3P_2 - 2s2p\ ^3P^o_2$ (△) and $2s2p\ ^1P^o_1 - 2s^2\ ^1S_0$ (∘), solid symbols: results of ZS92.The two separated points represent the infinite energy Born limit of collision strengths.

**Table 10:** Same as in Table 7 but for the Na VIII ion. ZS92 is the relativistic distorted wave calculations of Zhang & Sampson (1992). $\Delta = 100 \times \frac{|\text{Present}-\text{ZS92}|}{\text{ZS92}}$ (%).

| Trans. | $\varepsilon_1 = E_{ij} + 14.45$ | | | $\varepsilon_2 = E_{ij} + 30.44$ | | | $\varepsilon_3 = E_{ij} + 57.80$ | | | $\varepsilon_4 = E_{ij} + 101.2$ | | |
|---|---|---|---|---|---|---|---|---|---|---|---|---|
| $i-j$ | Present | ZS92 | Δ | Present | ZS92 | Δ | Present | ZS92 | Δ | Present | ZS92 | Δ |
| 1 −2 | 5.80E−03 | 5.29E−03 | 9 | 2.74E−03 | 2.68E−03 | 2 | 1.17E−03 | 1.18E−03 | 1 | 4.98E−04 | 5.04E−04 | 1 |
| 1 −3 | 1.75E−02 | 1.60E−02 | 9 | 8.38E−03 | 8.21E−03 | 2 | 3.68E−03 | 3.73E−03 | 1 | 1.69E−03 | 1.73E−03 | 2 |
| 1 −4 | 2.89E−02 | 2.64E−02 | 9 | 1.36E−02 | 1.33E−02 | 2 | 5.83E−03 | 5.87E−03 | 1 | 2.48E−03 | 2.50E−03 | 1 |
| 1 −6 | 1.82E−04 | 2.00E−04 | 10 | 7.70E−05 | 7.93E−05 | 3 | 2.70E−05 | 2.73E−05 | 1 | 1.00E−05 | 1.00E−05 | 0 |
| 1 −7 | 5.36E−04 | 5.90E−04 | 10 | 2.24E−04 | 2.29E−04 | 2 | 7.50E−05 | 7.37E−05 | 2 | 2.30E−05 | 2.23E−05 | 3 |
| 1 −8 | 9.02E−04 | 9.79E−04 | 9 | 3.92E−04 | 3.87E−04 | 1 | 1.48E−04 | 1.33E−04 | 10 | 6.30E−05 | 4.92E−05 | 22 |
| 1 −9 | 1.61E−02 | 9.99E−03 | 38 | 1.88E−02 | 1.16E−02 | 38 | 2.07E−02 | 1.29E−02 | 38 | 2.15E−02 | 1.36E−02 | 37 |
| 1 −10 | 3.33E−03 | 2.06E−03 | 38 | 3.39E−03 | 2.01E−03 | 41 | 3.36E−03 | 1.98E−03 | 41 | 3.31E−03 | 1.96E−03 | 41 |
| 2−3 | 5.79E−02 | 4.97E−02 | 14 | 2.53E−02 | 2.39E−02 | 6 | 1.03E−02 | 9.90E−03 | 4 | 4.21E−03 | 4.11E−03 | 3 |
| 2−4 | 6.06E−02 | 5.75E−02 | 5 | 5.66E−02 | 5.50E−02 | 3 | 5.68E−02 | 5.55E−02 | 2 | 5.77E−02 | 5.68E−02 | 2 |
| 2 −5 | 1.28E−02 | 1.05E−02 | 18 | 5.15E−03 | 4.71E−03 | 9 | 1.91E−03 | 1.77E−03 | 7 | 7.12E−04 | 6.70E−04 | 6 |
| 2 −6 | 3.45E−03 | 3.02E−03 | 12 | 1.59E−03 | 1.52E−03 | 4 | 6.68E−04 | 6.64E−04 | 1 | 2.80E−04 | 2.82E−04 | 1 |
| 2 −8 | 4.67E−03 | 4.04E−03 | 13 | 2.15E−03 | 2.02E−03 | 6 | 9.04E−04 | 8.87E−04 | 2 | 3.79E−04 | 3.76E−04 | 1 |
| 2 −9 | 8.57E−03 | 7.14E−03 | 17 | 3.96E−03 | 3.58E−03 | 10 | 1.66E−03 | 1.57E−03 | 5 | 6.97E−04 | 6.67E−04 | 4 |
| 2 −10 | 8.43E−04 | 6.90E−04 | 18 | 3.64E−04 | 3.29E−04 | 10 | 1.44E−04 | 1.35E−04 | 6 | 5.70E−05 | 5.36E−05 | 6 |
| 3 −4 | 2.09E−01 | 1.92E−01 | 8 | 1.59E−01 | 1.54E−01 | 3 | 1.41E−01 | 1.38E−01 | 2 | 1.35E−01 | 1.33E−01 | 1 |
| 3 −5 | 3.84E−02 | 3.19E−02 | 17 | 1.55E−02 | 1.40E−02 | 10 | 5.76E−03 | 5.43E−03 | 6 | 2.17E−03 | 2.07E−03 | 5 |
| 3 −9 | 2.66E−02 | 2.20E−02 | 17 | 1.24E−02 | 1.11E−02 | 10 | 5.24E−03 | 4.98E−03 | 5 | 2.39E−03 | 2.24E−03 | 6 |
| 3 −10 | 2.63E−03 | 2.16E−03 | 18 | 1.15E−03 | 1.04E−03 | 10 | 4.70E−04 | 4.51E−04 | 4 | 1.98E−04 | 2.08E−04 | 5 |
| 4−5 | 6.43E−02 | 5.30E−02 | 18 | 2.59E−02 | 2.37E−02 | 8 | 9.60E−03 | 9.03E−03 | 6 | 3.59E−03 | 3.40E−03 | 5 |
| 4 −6 | 4.14E−03 | 3.66E−03 | 12 | 1.91E−03 | 1.84E−03 | 4 | 8.05E−04 | 8.04E−04 | 0 | 3.38E−04 | 3.41E−04 | 1 |
| 4 −9 | 5.03E−02 | 4.16E−02 | 17 | 2.58E−02 | 2.35E−02 | 9 | 1.32E−02 | 1.36E−02 | 3 | 7.66E−03 | 9.51E−03 | 24 |
| 4 −10 | 4.62E−03 | 3.77E−03 | 18 | 2.00E−03 | 1.79E−03 | 11 | 7.96E−04 | 7.41E−04 | 7 | 3.15E−04 | 2.95E−04 | 6 |
| 5−6 | 5.92E−03 | 4.90E−03 | 17 | 2.89E−03 | 2.72E−03 | 6 | 1.36E−03 | 1.51E−03 | 11 | 7.23E−04 | 1.01E−03 | 40 |
| 5−7 | 1.78E−02 | 1.37E−02 | 23 | 7.86E−03 | 6.93E−03 | 12 | 3.24E−03 | 3.08E−03 | 5 | 1.37E−03 | 1.38E−03 | 1 |
| 6−7 | 7.38E−02 | 5.49E−02 | 26 | 3.03E−02 | 2.60E−02 | 14 | 1.20E−02 | 1.10E−02 | 8 | 4.85E−03 | 4.60E−03 | 5 |
| 6−8 | 6.17E−02 | 5.83E−02 | 6 | 5.49E−02 | 5.55E−02 | 1 | 5.46E−02 | 5.58E−02 | 2 | 5.53E−02 | 5.70E−02 | 3 |
| 6−9 | 3.91E−02 | 2.72E−02 | 30 | 1.42E−02 | 1.20E−02 | 15 | 5.03E−03 | 4.59E−03 | 9 | 1.82E−03 | 1.77E−03 | 3 |
| 6 −10 | 4.36E−03 | 3.11E−03 | 29 | 1.41E−03 | 1.19E−03 | 16 | 4.13E−04 | 3.79E−04 | 8 | 1.19E−04 | 1.16E−04 | 3 |
| 7−8 | 2.31E−01 | 1.99E−01 | 14 | 1.61E−01 | 1.57E−01 | 2 | 1.37E−01 | 1.38E−01 | 1 | 1.30E−01 | 1.34E−01 | 3 |
| 7−9 | 1.17E−01 | 8.22E−02 | 30 | 4.35E−02 | 3.64E−02 | 16 | 1.55E−02 | 1.39E−02 | 10 | 5.71E−03 | 5.34E−03 | 6 |
| 7 −10 | 1.33E−02 | 9.48E−03 | 29 | 4.29E−03 | 3.61E−03 | 16 | 1.26E−03 | 1.14E−03 | 10 | 3.64E−04 | 3.42E−04 | 6 |
| 8−9 | 1.95E−01 | 1.42E−01 | 93 | 7.54E−02 | 6.29E−02 | 17 | 2.74E−02 | 2.46E−02 | 10 | 1.05E−02 | 9.75E−03 | 7 |
| 8 −10 | 2.27E−02 | 1.61E−02 | 29 | 7.38E−03 | 6.18E−03 | 16 | 2.24E−03 | 2.00E−03 | 11 | 7.23E−04 | 6.53E−04 | 10 |
| 9 −10 | 1.53E−01 | 1.62E−01 | 6 | 1.72E−01 | 1.83E−01 | 6 | 1.89E−01 | 1.99E−01 | 5 | 1.98E−01 | 2.10E−01 | 6 |
| Avg. | | | 20 | | | 10 | | | 7 | | | 8 |

**Table 11:** Continued.

| Trans. | $\varepsilon_1 = E_{ij} + 14.45$ | | | $\varepsilon_2 = E_{ij} + 30.44$ | | | $\varepsilon_3 = E_{ij} + 57.80$ | | | $\varepsilon_4 = E_{ij} + 101.2$ | | |
|---|---|---|---|---|---|---|---|---|---|---|---|---|
| $i-j$ | Present | ZS92 | Δ | Present | ZS92 | Δ | Present | ZS92 | Δ | Present | ZS92 | Δ |
| 1 −5 | 2.27E+00 | 2.29E+00 | 1 | 2.42E+00 | 2.66E+00 | 10 | 2.32E+00 | 3.15E+00 | 36 | 2.11E+00 | 3.52E+00 | 67 |
| 2 −7 | 1.13E+00 | 1.22E+00 | 8 | 1.17E+00 | 1.46E+00 | 25 | 1.10E+00 | 1.67E+00 | 52 | 9.94E−01 | 1.85E+00 | 86 |
| 3 −6 | 1.13E+00 | 1.22E+00 | 8 | 1.32E+00 | 1.46E+00 | 11 | 1.39E+00 | 1.67E+00 | 20 | 1.34E+00 | 1.85E+00 | 38 |
| 3−7 | 8.57E−01 | 9.23E−01 | 8 | 8.82E−01 | 1.10E+00 | 25 | 8.05E−01 | 1.25E+00 | 52 | 7.46E−01 | 1.39E+00 | 86 |
| 2 −8 | 1.42E+00 | 1.53E+00 | 8 | 1.46E+00 | 1.83E+00 | 25 | 1.37E+00 | 2.09E+00 | 53 | 1.24E+00 | 2.32E+00 | 87 |
| 4 −7 | 1.42E+00 | 1.53E+00 | 8 | 1.46E+00 | 1.82E+00 | 25 | 1.37E+00 | 2.08E+00 | 52 | 1.24E+00 | 2.31E+00 | 86 |
| 4 −8 | 4.24E+00 | 4.57E+00 | 8 | 4.38E+00 | 5.47E+00 | 25 | 4.11E+00 | 6.25E+00 | 52 | 3.72E+00 | 6.94E+00 | 87 |
| 5 −10 | 1.42E+00 | 1.53E+00 | 14 | 1.46E+00 | 1.83E+00 | 30 | 1.37E+00 | 2.09E+00 | 58 | 1.24E+00 | 2.32E+00 | 94 |
| Avg. | | | 8 | | | 22 | | | 47 | | | 79 |

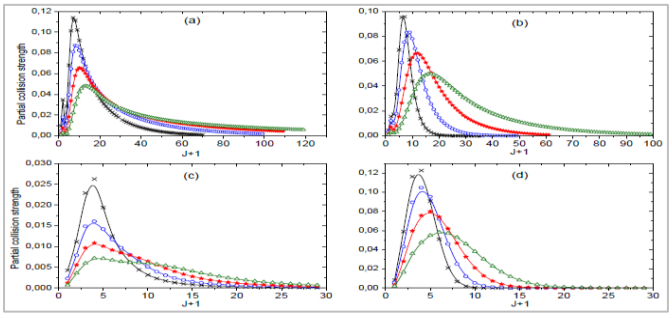


**Figure 2:** Na VII partial collision strength for the two allowed transitions: 6–1 (a) and 22–1 (b), and for the two forbidden ones: 2–1 (c) and 25–2 (d) at energies 30 Ryd (black-×), 60 Ryd (blue-∘), 120 Ryd (red-⋆) and 240 Ryd (green-△).

Since the collision strengths in intermediate coupling are given by the summation in the equation (5), it is important to ensure that we have included in that summation all the total angular momentum $J$ values that contribute to the collision strengths; i.e. check that the contributions of high $J$ decrease and approximately tend to zero. We have to see also that this convergence is ensured even for high electron energies. We performed this check and the results are displayed in Figs. 2 and 3. In Fig. 2, we present two Na VII allowed transitions $2s2p^2\ {}^2D_{3/2} - 2s\,{}^2 2p\ {}^2P^o_{1/2}$ (a :6–1) and $2s\,{}^2 3d\ {}^2D_{3/2} - 2s\,{}^2 2p\ {}^2P^o_{1/2}$ (b :22–1) and two forbidden ones $2s\,{}^2 2p\ {}^2P^o_{3/2} - 2s\,{}^2 2p\ {}^2P^o_{1/2}$ (c :2–1) and $2s2p(^3P)3s\ {}^2P^o_{3/2} - 2s\,{}^2 2p\ {}^2P^o_{3/2}$ (d :22–2).

We know that, in contrast to the forbidden transitions, the allowed ones do not converge faster with electron energy. We show in Fig. 2 that for the allowed transition (a:6–1), collision strengths converge even for high energy but we have to include higher angular momenta: $J \simeq 40$ at energy $\varepsilon = 30$ Ryd and $J \simeq 120$ at $\varepsilon = 240$ Ryd. The convergence of the allowed transition (b :22–1) is more faster ($J < 90$ at $\varepsilon = 240$ Ryd) because of the high energy difference of the transition (b :22–1): $\Delta_{22-1} \gg \Delta_{6-1}$. The collision strengths of the two forbidden transitions (c :2–1) and (d :22–2) converge very fast at low angular momenta $J = 10 - 20$. Same conclusions can be drawn for the Na VIII results displayed in Fig. 3. The allowed selected transitions are $2s2p\ {}^1P^o_1 - 2s^2\ {}^1S_0$ (a: 5–1), $2s3p\ {}^1P^o_1 - 2s\,{}^2 2p\ {}^2P^o_{1/2}$ (b :13–1) and the forbidden ones are $2s3d\ {}^1D_2 - 2s\,{}^2 2p\ {}^2P^o_{1/2}$ (c :20–1) and $2s3p\ {}^3P^o_2 - 2s\,{}^2 2p\ {}^2P^o_{3/2}$ (d :16–2).

In the light of the above discussions, three important conclusions can be drawn:

Our intermediate results (structural and collisional) agree well with several other calculations and measurements.

Our collision strengths converge for the considered electron energies, even at high energies and for allowed transitions.

The total angular momentum values are sufficiently included, so the collision calculation is complete.

Consequently, we conclude that our intermediate results are sufficiency accurate and complete to be used with confidence in the line broadening calculations.

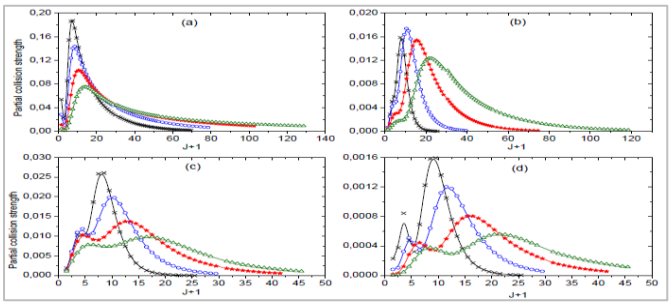


**Figure 3:** Na VIII partial collision strength for the two allowed transitions: 5–1 (a) and 13–1 (b), and for the two forbidden ones: 20–1 (c) and 16–2 (d) at energies 35 Ryd (black-×), 60 Ryd (blue-∘), 120 Ryd (red-⋆) and 240 Ryd (green-△).

### *3.2. Stark widths*

The method used in the JAJOM code to obtain the reactance matrices in intermediate coupling from those in *LS* coupling has been used long time ago, and it has been shown that it is adequate for ions of interest in our work. This transformation guarantees the introduction of the relativistic effects in the collision calculations. There are two types of relativistic effects [52]:

Corrections due to the motion of the scattered electron and its interaction with the emitter.

Corrections due to the non validity of the *LS* coupling approximation for the emitter.

It has been shown in Walker (1974) [53] that the contributions of the first type of corrections to cross sections do not exceed 10 % for ions with atomic number $Z \leq 25$. Consequently, they can be omitted in the present work. The second type is essential and they have been taken into account in our work. The method used in JAJOM to include these effects is justified by the high velocity of the scattered electrons. In fact, Jones (1974b) [54] showed that, in this case, we can omit the relativistic contribution to the Hamiltonian of the target when studying the collision. Hence, the reactance matrices can be evaluated for *LS* coupling firstly and then, they will be transformed into intermediate coupling using the (TCC) obtained for the atomic structure calculations including the relativistic effects.

We have performed Stark broadening calculations for 20 Na VII and 20 Na VIII lines, displayed respectively in Tables 12 and 13. The results have been presented at electron density $N_e = 10^{17}$ cm $^{-3}$ and for electron temperature ranging from $2\times 10^5$ K to $10^6$ K. There are no results in the literature to compare with. The obtained line widths can be useful for astrophysical and laboratory plasma diagnostics. New calculations or measurements of Stark broadeing for these two ions will be welcomed to check our results.

## 4. Conclusions

We have used in the present paper our quantum mechanical method to provide Stark broadening data for 20 Na VII and 20 Na VIII lines. The results are presented for a large range of electron temperature required for many astrophysical applications. Our method is ab initio, so we have calculated all the parameters needed (structure and collision data) for the line broadening evaluation. Since the accuracy of our line broadening results are related to that of the structure and collision data used in the calculations, it is important to check their accuracy. The structure study has been performed using the SUPERSTRUCTURE code [24]. The energy levels and their lifetimes of Na VII have been compared to the NIST [44] values, to the RCI ones Jönsson *et al.* [11], and to other relativistic (Koc) results [45]. Lifetimes are compared to the experimental values of Buchet *et al.* (1978)[46] and Tordoir *et al.* (1999) [47]. For Na VIII, the energy levels have been compared to the NIST [44], to the MCHF [10], to the Relativistic Many–Body [18] results (RMB) and to the Many–Body Perturbation Theory (MBPT) approach [12]. The agreement is good for the two ions and is less than 2 %. We calculated also radiative decay rates, oscillator strengths and line strengths. Extensive comparisons have been performed with the same references as for the energy levels, and we found an agreement of about 20 % for Na VII and about 7 % for Na VIII. The collision part has been treated using the UCL DISTORTED WAVE [25] and JAJOM [27] codes. We have calculated collision strengths between fine structure levels at four electron energies and we have compared them to the relativistic distorted wave results of Zhang & Sampson (1992, 1994) [20,21]. We found that the averaged agreement for Na VII is about 11 % and about 18 % for Na VIII, but found less agreement for transitions with high collision strengths. We show that for some of these transitions, the results of Zhang & Sampson (1992, 1994) [20,21] do not converge at high energy. This assertion and the difference between the configurations included in our calculations and those used in Zhang & Sampson (1992, 1994) [20,21] may be the origins of the disagreement found exceptionally for these transitions. We investigated also the convergence of our collision strengths with the electron energy, and we show that they converge even for high energies (up to 240 Ryd for Na VII and 300 Ryd for Na VIII). We selected two allowed transitions from each ion to show that their collision strengths converge also but for high total angular momentum $J$. It is known that collision strengths of this type of transitions do not converge easily with electron energy. The good agreements found between our calculations and all the other results for radiative atomic and collisional data show that our obtained results have high accuracy and hence, our line broadening data can be used with trust. To confirm this conclusion, new measurements or calculations of line widths using other approaches will be welcomed.

**Table 12:** Stark Widths for 20 Na VII lines at electron density $N_e = 10^{17}$ cm $^{-3}$. $T_e$ is given in $10^5$ K.

| Transition | $T_e$ | $W$(pm) | Transition | $W$(pm) | Transition | $W$(pm) |
|---|---|---|---|---|---|---|
| | 2 | 1.480−01 | | 6.320−02 | | 1.795−02 |
| $2s2p^2\ ^2D_{3/2} - 2s^2 2p\ ^2P^o_{1/2}$ | 4 | 1.097−01 | $2p^3\ ^2D^o_{3/2} - 2s2p^2\ ^2P_{1/2}$ | 4.790−02 | $2p^3\ ^2P^o_{3/2} - 2s2p^2\ ^2S_{1/2}$ | 1.316−02 |
| $\lambda$ =474.19 Å | 6 | 8.312−02 | $\lambda$ =791.35 Å | 4.079−02 | $\lambda$ =476.32 Å | 1.109−02 |
| 6 −1 | 8 | 6.547−02 | 12−9 | 3.640−02 | 15−8 | 9.855−03 |
| | 10 | 5.337−02 | | 3.329−02 | | 9.002−03 |
| | 2 | 1.204−01 | | 6.499−02 | | 3.691−03 |
| $2s2p^2\ ^2D_{3/2} - 2s^2 2p\ ^2P^o_{3/2}$ | 4 | 8.868−02 | $2p^3\ ^2D^o_{3/2} - 2s2p^2\ ^2P_{3/2}$ | 4.922−02 | $2s^2 3s\ ^2S_{1/2} - 2s^2 2p\ ^2P^o_{1/2}$ | 2.620−03 |
| $\lambda$ =479.17 Å | 6 | 6.731−02 | $\lambda$ =800.71 Å | 4.189−02 | $\lambda$ =103.30 Å | 2.140−03 |
| 6 −2 | 8 | 5.321−02 | 12−10 | 3.737−02 | 16−1 | 1.850−03 |
| | 10 | 4.358−02 | | 3.417−02 | | 1.651−03 |
| | 2 | 9.218−03 | | 6.422−02 | | 3.706−03 |
| $2s2p^2\ ^2S_{1/2} - 2s^2 2p\ ^2P^o_{1/2}$ | 4 | 6.953−03 | $2p^3\ ^2D^o_{5/2} - 2s2p^2\ ^2P_{3/2}$ | 4.872−02 | $2s^2 3s\ ^2S_{1/2} - 2s^2 2p\ ^2P^o_{3/2}$ | 2.631−03 |
| $\lambda$ =371.66 Å | 6 | 5.972−03 | $\lambda$ =800.39 Å | 4.151−02 | $\lambda$ =103.54 Å | 2.149−03 |
| 8 −1 | 8 | 5.391E−03 | 13−10 | 3.705E−02 | 16−2 | 1.858E−03 |
| | 10 | 4.989E−03 | | 3.390E−02 | | 1.658E−03 |
| | 2 | 9.310E−03 | | 1.099E−01 | | 9.404E−03 |
| $2s2p^2\ ^2S_{1/2} - 2s^2 2p\ ^2P^o_{3/2}$ | 4 | 7.029E−03 | $2p^3\ ^2P^o_{1/2} - 2s2p^2\ ^2D_{3/2}$ | 7.502E−02 | $2s^2 3p\ ^2P^o_{1/2} - 2s2p^2\ ^2D_{3/2}$ | 5.584E−03 |
| $\lambda$ =374.72 Å | 6 | 6.042E−03 | $\lambda$ =373.19 Å | 5.486E−02 | $\lambda$ =122.45 Å | 4.113E−03 |
| 8 −2 | 8 | 5.457E−03 | 14−6 | 4.240E−02 | 17−6 | 3.329E−03 |
| | 10 | 5.052E−03 | | 3.412E−02 | | 2.837E−03 |
| | 2 | 7.774E−03 | | 8.719E−02 | | 8.105E−03 |
| $2p^3\ ^4S^o_{3/2} - 2s2p^2\ ^4P^o_{1/2}$ | 4 | 5.558E−03 | $2p^3\ ^2P^o_{3/2} - 2s2p^2\ ^2D_{3/2}$ | 5.932E−02 | $2s^2 3p\ ^2P^o_{3/2} - 2s2p^2\ ^2D_{3/2}$ | 4.977E−03 |
| $\lambda$ =389.91 Å | 6 | 4.602E−03 | $\lambda$ =372.97 Å | 4.351E−02 | $\lambda$ =122.37 Å | 3.744E−03 |
| 11 −3 | 8 | 4.034E−03 | 15−6 | 3.378E−02 | 18−6 | 3.073E−03 |
| | 10 | 3.642E−03 | | 2.735E−02 | | 2.645E−03 |
| | 2 | 7.674E−03 | | 7.595E−02 | | 6.615E−03 |
| $2p^3\ ^4S^o_{3/2} - 2s2p^2\ ^4P^o_{3/2}$ | 4 | 5.498E−03 | $2p^3\ ^2P^o_{3/2} - 2s2p^2\ ^2D_{5/2}$ | 5.220E−02 | $2s^2 3p\ ^2P^o_{3/2} - 2s2p^2\ ^2D_{5/2}$ | 4.275E−03 |
| $\lambda$ =391.09 Å | 6 | 4.559E−03 | $\lambda$ =373.01 Å | 3.823E−02 | $\lambda$ =122.38 Å | 3.317E−03 |
| 11 −4 | 8 | 4.002E−03 | 15−7 | 2.966E−02 | 18−7 | 2.778E−03 |
| | 10 | 3.617E−03 | | 2.403E−02 | | 2.425E−03 |
| | 2 | 7.469E−03 | | 1.802E−02 | | |
| $2p^3\ ^4S^o_{3/2} - 2s2p^2\ ^4P^o_{5/2}$ | 4 | 5.372E−03 | $2p^3\ ^2P^o_{1/2} - 2s2p^2\ ^2S_{1/2}$ | 1.321E−02 | | |
| $\lambda$ =393.03 Å | 6 | 4.470E−03 | $\lambda$ =476.67 Å | 1.113E−02 | | |
| 11 −5 | 8 | 3.933E−03 | 14−8 | 9.888E−03 | | |
| | 10 | 3.562E−03 | | 9.031E−03 | | |

**Table 13:** Stark Widths for 20 Na VIII lines at electron density $N_e = 10^{17}$ cm $^{-3}$. $T_e$ is given in $10^5$ K.

| Transition | $T_e$ | $W$(pm) | Transition | $W$(pm) | Transition | $W$(pm) |
|---|---|---|---|---|---|---|
| | 2 | 1.491E−02 | | 1.627E−03 | | 1.661E−02 |
| 2s2p $^1P^o_1 - 2s^2\ ^1S_0$ | 4 | 1.099E−02 | 2s3p $^1P^o_1 - 2s^2\ ^1S_0$ | 1.147E−03 | 2s3d $^3D_2 - 2s2p\ ^3P^o_1$ | 1.105E−02 |
| $\lambda$ =396.05 Å | 6 | 9.351E−03 | $\lambda$ =77.2 Å | 9.356E−04 | $\lambda$ =83.34 Å | 8.341E−03 |
| 5 −1 | 8 | 8.408E−03 | 13−1 | 8.095E−04 | 18−3 | 6.708E−03 |
| | 10 | 7.767E−03 | | 7.231E−04 | | 5.613E−03 |
| | 2 | 1.341E+00 | | 8.259E−03 | | 1.572E−02 |
| 2p $^2\ ^1D_2 - 2s2p\ ^1P^o_1$ | 4 | 7.798E−01 | 2s3p $^1P^o_1 - 2p^2\ ^1D_2$ | 5.219E−03 | 2s3d $^3D_2 - 2s2p\ ^3P^o_2$ | 1.048E−02 |
| $\lambda$ =851.72 Å | 6 | 5.381E−01 | $\lambda$ =108.19 Å | 3.867E−03 | $\lambda$ =83.45 Å | 7.930E−03 |
| 9 −5 | 8 | 4.063E−01 | 13−9 | 3.093E−03 | 18−4 | 6.393E−03 |
| | 10 | 3.239E−01 | | 2.591E−03 | | 5.360E−03 |
| | 2 | 2.253E−02 | | 4.071E−03 | | 1.232E−02 |
| 2p $^2\ ^1S_0 - 2s2p\ ^1P^o_1$ | 4 | 1.665E−02 | 2s3p $^1P^o_1 - 2p^2\ ^1S_0$ | 2.877E−03 | 2s3d $^3D_3 - 2s2p\ ^3P^o_2$ | 8.062E−03 |
| $\lambda$ =480.95 Å | 6 | 1.422E−02 | $\lambda$ =119.94 Å | 2.352E−03 | $\lambda$ =83.44 Å | 5.970E−03 |
| 10 −5 | 8 | 1.281E−02 | 13−10 | 2.040E−03 | 19−4 | 4.715E−03 |
| | 10 | 1.184E−02 | | 1.826E−03 | | 3.881E−03 |
| | 2 | 2.385E−03 | | 3.147E+00 | | 1.226E−01 |
| 2p3s $^3S_1 - 2s2p\ ^3P^o_0$ | 4 | 1.693E−03 | 2s3p $^1P^o_1 - 2s3s\ ^1S_0$ | 2.519E+00 | 2p3s $^3P^o_0 - 2s3s\ ^3S_1$ | 8.614E−02 |
| $\lambda$ =89.95 Å | 6 | 1.383E−03 | $\lambda$ =119.94 Å | 2.172E+00 | $\lambda$ =617.81 Å | 6.954E−02 |
| 11 −2 | 8 | 1.194E−03 | 13−12 | 1.934E+00 | 21−11 | 5.955E−02 |
| | 10 | 1.062E−03 | | 1.757E+00 | | 5.268E−02 |
| | 2 | 2.387E−03 | | 2.014E−02 | | 6.439E−03 |
| 2p3s $^3S_1 - 2s2p\ ^3P^o_1$ | 4 | 1.695E−03 | 2s3d $^3D_1 - 2s2p\ ^3P^o_0$ | 1.347E−02 | 2p3s $^1P^o_1 - 2p^2\ ^1D_2$ | 4.075E−03 |
| $\lambda$ =90.02 Å | 6 | 1.384E−03 | $\lambda$ =83.28 Å | 1.025E−02 | $\lambda$ =94.54 Å | 3.043E−03 |
| 11 −3 | 8 | 1.195E−03 | 17−2 | 8.293E−03 | 24−9 | 2.456E−03 |
| | 10 | 1.063E−03 | | 6.979E−03 | | 2.075E−03 |
| | 2 | 2.390E−03 | | 2.016E−02 | | 4.438E−03 |
| 2p3s $^3S_1 - 2s2p\ ^3P^o_2$ | 4 | 1.697E−03 | 2s3d $^3D_1 - 2s2p\ ^3P^o_1$ | 1.349E−02 | 2p3s $^1P^o_1 - 2p^2\ ^1S_0$ | 3.076E−03 |
| $\lambda$ =90.16 Å | 6 | 1.387E−03 | $\lambda$ =83.34 Å | 1.026E−02 | $\lambda$ =103.39 Å | 2.467E−03 |
| 11 −4 | 8 | 1.197E−03 | 17−3 | 8.304E−03 | 24−10 | 2.103E−03 |
| | 10 | 1.065E−03 | | 6.988E−03 | | 1.855E−03 |
| | 2 | 3.208E−03 | | 1.685E−02 | | |
| 2p3s $^1S_0 - 2s2p\ ^1P^o_1$ | 4 | 2.276E−03 | 2s3d $^3D_1 - 2s2p\ ^3P^o_2$ | 1.128E−02 | | |
| $\lambda$ =98.99 Å | 6 | 1.859E−03 | $\lambda$ =83.46 Å | 8.586E−03 | | |
| 12 −5 | 8 | 1.608E−03 | 17−4 | 6.960E−03 | | |
| | 10 | 1.435E−03 | | 5.867E−03 | | |

**Acknowledgments:** The author is grateful to Prof. Sylvie Sahal-Bréchot for several fruitful discussions. This work has been supported by the Tunisian Laboratory of Molecular Spectroscopy and Dynamics LR18ES02.

**Conflicts of Interest:** Declare conflicts of interest or state "The authors declare no conflict of interest."

**References**

[1] T. Rauch *et al*. Stellar laboratories. IX. New Se V, Sr IV-VII, Te VI, and I VI oscillator strengths and the Se, Sr, Te, and I abundances in the hot white dwarfs G191-B2B and RE 0503-289. *A&A*. **2017**, *606*, A105-132. https://doi.org/10.1051/0004-6361/201730383

[2] M. S. Dimitrijević. Stark broadening in asyrophysics (Applications of Belgrade school results and collaboration with former Soviet republics). *Astronomical & Astrophysical Transactions*. **2003**, *22*, 389-412. https://doi.org/10.1080/1055679031000108167

[3] A. E. Lynas-Gray *et al*. Current State of Astrophysical Opacities : A White Paper. Astronomical Society of the Pacific Conference Series. **2018,** 301-318 (arXiv:1804.06804)

[4] K. Werner, T. Rauch, M. Knörzer and J. W. Kruk. First detection of bromine and antimony in hot stars. *A&A*. **2018,** *614*, A96-100. https://doi.org/10.1051/0004-6361/201832723

[5] D. R. Flower and H. Nussbaumer. On the extreme ultraviolet solar emission of B-like ions: O IV. *A&A*. **1975a**, *45*, 145-150. https://doi.org/10.1051/0004-6361:200811222

[6] D. R. Flower and H. Nussbaumer. On the extreme ultraviolet solar emission of B-like ions: Na VII, Si X and S XII. *A&A*. **1975b**, *45*, 349-352. https://doi.org/10.1051/0004-6361:200811222

[7] D. L. McKenzie, P. B. Landecker, U. Feldman and G. A. Doschek. The solar coronal X-ray spectrum from 5.5 to 12 Å. *ApJ*. **1985**, *289*, 849-857. 10.1086/162949

[8] B. C . Fawcett, K. J. H. Phillips, C. Jordan and J. R. Lemen. New spectral line identifications in high-temperature flares. *MNRAS*. **1987**, *225*, 1013-1023. https://doi.org/10.1093/mnras/225.4.1013

[9] J. P. Marques *et al*. Theoretical determination of K X-ray transition energy and probability values for highly charged (He-through B-like) Nd, Sm, Gd, Dy, Er, and Yb ions. *Radiation Physics and Chemistry*. **2019**, *154*, 17-20. https://doi.org/10.1016/j.radphyschem.2018.02.003

[10] C. Froese Fischer and G. Tachiev. Breit-Pauli energy levels, lifetimes, and transition probabilities for the beryllium-like to neon-like sequences. *At. Data Nucl. Data Tables.* **2004**, *87*, 1-184. https://doi.org/10.1016/j.adt.2004.02.001

[11] P. Jönsson, J. Ekman and E. Träbert. MCDHF Calculations and Beam-Foil EUV Spectra of Boron-Like Sodium Ions (Na VII). *Atoms*. **2015**, *3*, 195-259. https://doi.org/10.3390/atoms3020195

[12] K. Wang *et al*. Systematic calculations of energy of levels and transition rates of be-like ions with $Z$ =10–30 using a combined configuration interaction and many-body perturbation theory approach. *ApJS.* **2015**, *218*, 16-29. https://doi.org/10.1088/0067-0049/218/2/16

[13] A. E. Kingston and A. Hibbert. Breit-Pauli calculations of the energy levels and oscillator strengths of Be-like ions. *J. Phys. B: At. Mol. Opt. Phys.* **2000**, *33*, 693-708. https://doi.org/10.1088/0953-4075/33/4/307

[14] A. E. Kingston and A. Hibbert. Breit-Pauli calculations of the Einstein rate coefficients for magnetic dipole, electric quadrupole and magnetic quadrupole transitions in Be-like ions. *J. Phys. B: At. Mol. Opt. Phys.* **2001**, *34*, 81-98. https://doi.org/10.1088/0953-4075/34/1/307

[15] M. F. Gu. Energies of 1s $^2$2l $^q$ ($1 \leqslant q \leqslant 8$) states for $Z \leqslant 60$ with a combined configuration interaction and many-body perturbation theory approach. *At. Data Nucl. Data Tables*. **2005a**, *89*, 267-293. https://doi.org/10.1016/j.adt.2005.02.004

[16] M. F. Gu. Wavelengths of 2l-->3l' Transitions in L-Shell Ions of Iron and Nickel: A Combined Configuration Interaction and Many-Body Perturbation Theory Approach. *ApJS.* **2005b**, *156*, 105-110. https://doi.org/10.1086/425915

[17] M. Andersson, Y. Zou, R. Hutton and T. Brage. Hyperfine-dependent lifetimes in Be-like ions. *Phys. Rev. A.* **2009**, *79*, 032501. https://doi.org/10.1103/PhysRevA.79.032501

[18] M. S. Safronova, W. R. Johnson and U. I. Safronova. Relativistic many-body calculations of energies of n = 3 states of Be-like ions. *J. Phys. B: At. Mol. Opt. Phys.* **1997**, *30*, 2375-2393. https://doi.org/10.1088/0953-4075/30/10/012

[19] U. IK. Safronova, A. Derevianko, M. S. Safronova and W. R. Johnson. Relativistic many-body calculations of transition probabilities for the $2l_12l_2$[LSJ]- $2l_33l_4$[L'S'J'] lines in Be-like ions. *J. Phys. B: At. Mol. Opt. Phys.* **1999**, *32*, 3527-3545. https://doi.org/10.1238/Physica.Regular.059a00286

[20] H. L. Zhang and D. H. Sampson. Relativistic Distorted-Wave Collision Strengths and Oscillator Strengths for the 105 Δn = 0 Transitions with n = 2 in the 85 B-Like Ions with 8 <= Z <= 92. *At. Data Nucl. Data Tables.* **1994**, *56*, 41-104. https://doi.org/10.1006/adnd.1994.1002

[21] H. L. Zhang and D. H. Sampson. Relativistic Distorted-Wave Collision Strengths and Oscillator Strengths for the 45 Δn =0 Transitions with n = 2 in the 85 Be-like Ions with 8 <= Z <= 92. *At. Data Nucl. Data Tables*. **1992**, *52*, 143-173. https://doi.org/10.1016/0092-640X(92)90011-6

[22] G. Y. Liang, N. R. Badnell and G. Zhao. R-matrix electron-impact excitation data for the B-like iso-electronic sequence. *A&A.* **2012**, *547*, A87-99. https://doi.org/10.1051/0004-6361/201220277

[23] L. Fernández-Menchero, G. Del Zanna and N. R. Badnel. R-matrix electron-impact excitation data for the Be-like iso-electronic sequence. *A&A.* **2014**, *566*, A104-115. https://doi.org/10.1051/0004-6361/201423864

[24] W. Eissner, M. Jones and H. Nussbaumer. Techniques for the calculation of atomic structures and radiative data including relativistic corrections. *Comput. Phys. Commun.* **1974**, *8*, 270-306. https://doi.org/10.1016/0010-4655(74)90019-8

[25] W. Eissner. The UCL distorted wave code. *Comput. Phys. Commun.* **1998**, *114*, 295-341. https://doi.org/10.1016/S0010-4655(98)00082-4

[26] H. E. Saraph. Fine structure cross sections from reactance matrices. *Comput. Phys. Commun.* **1972**, *3*, 256-268. https://doi.org/10.1016/0010-4655(72)90071-9
[27] H. E. Saraph. Fine structure cross sections from reactance matrices, a more versatile development of the program JAJOM. *Comput. Phys. Commun.* **1978**, *15*, 247-258. https://doi.org/10.1016/0010-4655(78)90095-4
[28] H. Elabidi, N. Ben Nessib and S. Sahal-Bréchot. Quantum mechanical calculations of the electron-impact broadening of spectral lines for intermediate coupling. *J. Phys. B: At. Mol. Opt. Phys.* **2004**, *37*, 63-71. https://doi.org/10.1088/0953-4075/37/1/004
[29] H. Elabidi, N. Bennessib, M. Cornille, J. Dubau and S. Sahal-Bréchot. Electron impact broadening of spectral lines in Be-like ions: quantum calculations. *J. Phys. B: At. Mol. Opt. Phys.* **2008**, *41*, n°025702. https://doi.org/10.1088/0953-4075/41/2/025702
[30] H. Elabidi, N. Ben Nessib and S. Sahal-Bréchot. Quantum Stark broadening of 3s–3p spectral lines in Li-like ions; Z-scaling and comparison with semi-classical perturbation theory. *Eur. Phys. J. D.* **2009**, *54*, 51-64. https://doi.org/10.1140/epjd/e2009-00167-8
[31] H. Elabidi and S. Sahal-Bréchot. Checking the dependence on the upper level ionization potential of electron impact widths using quantum calculations. *Eur. Phys. J. D.* **2011**, *61*, 285-290. https://doi.org/10.1140/epjd/e2010-10298-4
[32] H. Elabidi, S. Sahal-Bréchot and M. S. Dimitrijević. Quantum Stark broadening of Ar XV lines. Strong collision and quadrupolar potential contributions. *Adv. Space Res.* **2014**, *54*, 1184-1189. https://doi.org/10.1016/j.asr.2013.08.017
[33] R. Aloui, H. Elabidi, S. Sahal-Bréchot and M. S. Dimitrijević. Quantum and semiclassical Stark widths for Ar VII spectral lines. *Atoms.* **2018**, *6*, 20-34. https://doi.org/10.3390/atoms6020020
[34] H. Elabidi and S. Sahal-Bréchot. Quantum mechanical Stark widths for Ar V and Ar VI lines: scaling with temperature. *MNRAS.* **2018**, *480*, 697-706. https://doi.org/10.1093/mnras/sty1858
[35] H. Elabidi and S. Sahal-Bréchot. Stark line widths for N-like ions Na V, Mg VI, Al VII and Si VIII. Z–scaling. *MNRAS*. **2019**, *484*, 1072-1078. https://doi.org/10.1093/mnras/stv1970
[36] R. Aloui, H. Elabidi, R. Hamdi and S. Sahal-Bréchot. Quantum Stark broadening data for Ar VIII and Ar IX lines. *MNRAS*. **2019**, *484*, 4801-4810. https://doi.org/10.1093/mnras/stz303
[37] M. S. Dimitrijević and S. Sahal-Bréchot. Stark Broadening Parameter Tables for Ar VIII. *Serb. Astron. J.* **1999**, *160*, 15-20.
[38] E. U. Condon and G. H. Shortley. The theory of atomic spectra. Cambridge University Press. London. **1959**
[39] H. A. Bethe and E. E. Salpeter. Quantum Mechanics of One–and Two–Electron Atoms. Springer, Berlin, Göttingen. **1957**. 10.1007/978-3-662-12869-5
[40] M. Jones. Relativistic corrections to atomic energy levels. *J. Phys. B: At. Mol. Phys.* **1970**, *3*, 1571-1592. https://doi.org/10.1088/0022-3700/3/12/003
[41] M. Jones. Mutual spin-orbit and spin-spin interactions in atomic structure calculations. *J. Phys. B: At. Mol. Phys*. **1971**, *4*, 1422-1439. https://doi.org/10.1088/0022-3700/4/11/006
[42] G. Racah. Theory of Complex Spectra. III. *Phys. Rev.* **1943**, *63*, 367-382. https://doi.org/10.1103/PhysRev.63.367
[43] M. Baranger. General Impact Theory of Pressure Broadening. *Phys. Rev.* **1958**, *112*, 855-865. https://doi.org/10.1103/PhysRev.112.855
[44] A. Kramida *et al.* (accessed July 25, 2018), NIST Atomic Spectra Database (ver. 5.5.6), **2018** , https://physics.nist.gov/ asd
[45] K. Koc. Relativistic MR RCI Calculation of Energy Levels and Transition Probabilities of Boron Isoelectronic Sequence. *Phys. Scr.* **2003**, *67*, 491-499. https://doi.org/10.1238/Physica.Regular.067a00491
[46] J. P. Buchet, M. C. Buchet-Poulizac, and M. Druetta. Mean-life measurements of Na V, Na VI and Na VII levels in the extreme ultraviolet region. *Phys. Scr.* **1978**, *18*, 496-498. https://doi.org/10.1088/0031-8949/18/6/029
[47] X. Tordoir *et al*. Atomic lifetimes and transition probabilities in boron-like (Na VII) and beryllium-like (Na VIII) sodium ions. *Eur. Phys. J. D.* **1999**, *6*, 1-7. https://doi.org/10.1007/PL00021604
[48] D. E. Kelleher and L. I. Podobedova. Atomic Transition Probabilities of Sodium and Magnesium. A Critical Compilation. *J. Phys. Chem. Ref. Data*. **2008**, *37*, 267-706. https://doi.org/10.1063/1.2735328
[49] A. Burgess and V. B. Sheorey. Electron impact excitation of the resonance lines of alkali-like positive ions. *J. Phys. B: At. Mol. Phys.* **1974**, *7*, 2403-2416. https://doi.org/10.1088/0022-3700/7/17/026
[50] M. C. Chidichimo and S. P. Haigh. Electron-impact excitation of quadrupole-allowed transitions in positive ions. *Phys. Rev. A.* **1989**, *39*, 4991-4997. 10.1103/physreva.39.4991
[51] M. C. Chidichimo. Electron-impact excitation of electric octupole transitions in positive ions: Asymptotic behavior of the sum over partial-collision strengths. *Phys. Rev. A.* **1992**, *45*, 1690-1700. https://doi.org/10.1103/PhysRevA.45.1690
[52] M. Jones. Application of the Breit-Pauli approximation to the study of relativistic effects in electron-atom scattering. *J. Phys. B: At. Mol. Phys.* **1974a**, *7*, L284-285. https://doi.org/10.1088/0022-3700/7/9/003
[53] D. W. Walker. Electron impact excitation of hydrogenic ions. *J. Phys. B: At. Mol. Phys.* **1974**, *7*, 97-116. https://doi.org/10.1088/0022-3700/8/5/010
[54] M. Jones, M. Collision strengths for the electron-impact excitation of certain highly-ionized helium-like ions. *MNRAS*, **1974b**, *169*, 211-228. https://doi.org/10.1093/mnras/169.2.211